The effect of orientation on heat transfer coefficients in a fluidized bed : bare and finned tubes
by Rodney August Schmall

A thesis submitted to the Graduate Faculty in partial fulfillment of the requirements for the degree of
MASTER OF SCIENCE in Chemical Engineering
Montana State University
© Copyright by Rodney August Schmall (1970)

Abstract:
The objective of this study was to determine the effect of orientation on heat transfer coefficients of single care and finned tubes in a fluidized bed.

Bare and finned tubes were studied at five angles each: 0°, 30° , 45° , 60°, and 90° with respect to the horizontal. Studies were made in a 12-in. diameter plastic vessel using three sizes of glass beads as the bed: .0185, .0080, and .0045 in. in diameter.

Heat was supplied by the use of electrical heaters inserted inside the tubes.

It was found that in the case of the finned tube, the heat transfer coefficients in the vertical position were approximately 15 to 2O% lower than the coefficients in the horizontal position. Effectiveness factors of the finned tube were between 0.1 and O.4.

Bare tube coefficients were found less sensitive to orientation. However, a minimum value was observed at 45° for each particle size. The orders of magnitude of the coefficients of the bare tube were found to agree quite well with the data obtained by other investigators.

For the finned, tube, the particle Nusselt numbers were correlated with the following equation: (Formula not captured by OCR) where C is a function of angle and DP is exnressed in inches.

For the bare tube the correlation was found to be: (Formula not captured by OCR) where DP is expressed in inches.

Statement of Permission to Copy

In presenting this thesis in partial fulfillment of the requirements for an advanced degree at Montana State University, I agree that the Library shall make it freely available for inspection. I further agree that permission for extensive copying of this thesis for scholarly purposes may be granted by my major professor, or, in his absence, by the Director of Libraries. It is understood that any copying or publication of this thesis for financial gain shall not be allowed without my written permission.

Signature Rodney A. Schmidt

Date February 27, 1970

THE EFFECT OF ORIENTATION ON HEAT TRANSFER COEFFICIENTS IN A FLUIDIZED BED -- BARE AND FINNED TUBES

by 1151

RODNEY AUGUST SCHMALL

A thesis submitted to the Graduate Faculty in partial fulfillment of the requirements for the degree

of

MASTER OF SCIENCE

in

Chemical Engineering

Approved:

Lloyd Berg
Head, Major Department

William C. Benitti
Chairman, Examining Committee

D. Goering
Graduate Dean

MONTANA STATE UNIVERSITY
Bozeman, Montana

March, 1970

ACKNOWLEDGMENTS

I would like to thank Dr. William Genetti of Montana State University and Mr. Earl Grimmett of Idaho Nuclear Corporation for their assistance which helped me to complete this research project. Special thanks go to Dr. Genetti and Mr. Bill Bartel for their encouragement throughout the period of research.

I wish to acknowledge the financial support I received from Idaho Nuclear Corporation and the Atomic Energy Commission. Gratitude is extended to Associated Western Universities for handling the fellowship funds.

ABSTRACT

The objective of this study was to determine the effect of orientation on heat transfer coefficients of single bare and finned tubes in a fluidized bed.

Bare and finned tubes were studied at five angles each: 0°, 30°, 45°, 60°, and 90° with respect to the horizontal. Studies were made in a 12-in. diameter plastic vessel using three sizes of glass beads as the bed: .0185, .0080, and .0045 in. in diameter. Heat was supplied by the use of electrical heaters inserted inside the tubes.

It was found that in the case of the finned tube, the heat transfer coefficients in the vertical position were approximately 15 to 20% lower than the coefficients in the horizontal position. Effectiveness factors of the finned tube were between 0.1 and 0.4.

Bare tube coefficients were found less sensitive to orientation. However, a minimum value was observed at 45° for each particle size. The orders of magnitude of the coefficients of the bare tube were found to agree quite well with the data obtained by other investigators.

For the finned tube, the particle Nusselt numbers were correlated with the following equation:

$$Nu = \frac{11\,(1-\epsilon)^{1/2}}{\left[1 + \dfrac{C}{Re^{.51}\left(\dfrac{D_p}{.008}\right)^{.35}}\right]^2}$$

where C is a function of angle and D_p is expressed in inches.

For the bare tube the correlation was found to be:

$$Nu = \frac{11\,(1-\epsilon)^{1/2}}{\left[1 + \dfrac{.44 - .20(\theta-45)^2}{\dfrac{(\theta-45)^2 + 120}{Re^{.24}\left(\dfrac{D_p}{.008}\right)^{1.23}}}\right]^2}$$

where D_p is expressed in inches.

TABLE OF CONTENTS

	PAGE
LIST OF TABLES	vii
LIST OF FIGURES	viii
INTRODUCTION	1
THEORY AND LITERATURE SURVEY	5
Proposed Models for Fluidized Bed Heat Transfer	5
Experimental Studies of Fluidized Bed Heat Transfer	8
EXPERIMENTAL APPARATUS	11
EXPERIMENTAL PROGRAM	20
EXPERIMENTAL PROCEDURE	24
CALCULATIONS	27
DEVELOPMENT OF CORRELATIONS	32
Bare Tube	33
Finned Tube	38
RESULTS AND CONCLUSIONS	50
Results and Discussion	50
Sources of Error	71
Conclusions	73
BIBLIOGRAPHY	76

TABLE OF CONTENTS (continued)

	PAGE
APPENDIX	78
NOMENCLATURE	79
COMMENTS	83
EQUIPMENT	84
SAMPLE DATA SHEET	86
DEVELOPMENT OF TEMPERATURE OF AVERAGE FOR FINNED TUBE	87
PARTICLE FRACTION	89
Q/Δ T VALUES FROM ARBITRARY COEFFICIENTS USING AN ANALYTICAL PROCEDURE	90
COEFFICIENTS FROM CORRELATIONS FOR HORIZONTAL BARE TUBE	91
COEFFICIENTS FROM CORRELATION FOR VERTICAL BARE TUBE	92
EFFECTIVENESS FACTORS	93
PREDICTED EFFECT OF ANGLE	95
RECORDED AND CALCULATED DATA	96

LIST OF TABLES

TABLE		PAGE
I	COMPARISON OF EXPERIMENTAL VALUES OF G_{mf} AND VALUES PREDICTED BY LEVA'S EQUATION	50
II	COMPARISON OF DATA FROM CORRELATIONS AND EXPERIMENT	55

LIST OF FIGURES

FIGURE		PAGE
1	PHOTOGRAPH OF APPARATUS	14
2	PHOTOGRAPH OF TUBES AND HEATER	15
3	SKETCH OF APPARATUS	16
4	DRAWING OF TUBES AND HEATER	17
5	SKETCH OF RACK	18
6	ANGLES INVESTIGATED	21
7	PLOT OF LOG F VERSUS LOG Re FOR BARE TUBE	34
8	PLOT OF LOG $\frac{F}{Re^a}$ VERSUS LOG $\frac{D_p}{.008}$ FOR BARE TUBE	36
9	PLOT OF C VERSUS ANGLE FOR BARE TUBE	37
10	DIFFERENTIAL ELEMENT IN FIN	39
11	PLOT OF $Q/\Delta T$ VERSUS h	44
12	PLOT OF LOG F VERSUS LOG Re FOR FINNED TUBE	47
13	PLOT OF LOG $\frac{F}{Re^a}$ VERSUS LOG $\frac{D_p}{.008}$ FOR FINNED TUBE	48
14	PLOT OF C VERSUS ANGLE FOR FINNED TUBE	49
15	COMPARISON OF PREDICTED AND EXPERIMENTAL MINIMUM FLUIDIZATION VELOCITIES	51
16	RESULTS OF BARE TUBE STUDY	53

LIST OF FIGURES (continued)

FIGURE		PAGE
17	COMPARISON OF HORIZONTAL BARE TUBE CO-EFFICIENTS AND PREDICTED VALUES	56
18	COMPARISON OF VERTICAL BARE TUBE CO-EFFICIENTS AND PREDICTED VALUES	57
19	COMPARISON OF EXPERIMENTAL Nu's AND THE AUTHOR'S CORRELATION (BARE TUBE)	59
20	COMPARISON OF EXPERIMENTAL h_b's AND PREDICTED VALUES FROM THE AUTHOR'S CORRELATION (BARE TUBE)	60
21	PREDICTED EFFECT OF ANGLE ON HEAT TRANSFER COEFFICIENTS OF BARE TUBE	61
22	RESULTS OF h_{ff} FROM FINNED TUBE STUDY	63
23	RESULTS OF h_f FROM FINNED TUBE STUDY	64
24	RESULTING EFFECTIVENESS FACTORS FROM BARE AND FINNED TUBE STUDIES	66
25	COMPARISON OF EXPERIMENTAL Nu's AND THE AUTHOR'S CORRELATION (FINNED TUBE)	68
26	COMPARISON OF EXPERIMENTAL h_f's AND PREDICTED VALUES FROM THE AUTHOR'S CORRELATION (FINNED TUBE)	69
27	PREDICTED EFFECT OF ANGLE ON HEAT TRANSFER COEFFICIENTS OF FINNED TUBE	70
28	EFFECT OF INCREASED THERMAL CONDUCTIVITY ON HEAT TRANSFER	72

INTRODUCTION

Since the development of the fluidized bed catalytic cracker for petroleum, fluidized beds have been used with success in other operations and processes. The success of this first major industrial use of a fluidized bed created interest in the United States and elsewhere. As a result, fluidized bed technology has been expanding rapidly since 1940.

A definition of fluidization given by Kunii and Levenspiel (6) is "... the operation by which fine solids are transformed into a fluidized state through contact with a gas or a liquid." Thus, a fluidized bed is merely a mass of particles given fluid-like properties by a moving fluid.

Applications of fluidized beds are mainly of two types: (1) chemical change and catalysis, and (2) physical and mechanical processes. The latter type is used more extensively than the first. The first type includes fluid cracking, coking operations, and many catalytic processes. Physical applications include drying, blending, conveying, calcining, and energy transfer. Many uses involve both the chemical and physical aspects of fluidized bed technology.

The main characteristic of a fluidized bed which makes it applicable in many difficult operations is that uniform conditions

exist throughout the bed due to vigorous particle mixing. Temperatures vary only slightly in a fluidized bed involving heat transfer. This permits reactions which are very sensitive to temperature to take place. Because of particle mixing, concentrations of components in a solution can also be kept uniform during a chemical or physical process by using fluidization. By reducing temperature or concentration gradients, the driving forces for heat and mass transfer are kept from decreasing.

Uses of fluidization for many purposes have been and continue to be studied. In this investigation, gas fluidization involving heat transfer was examined.

Chemical and physical processes in which fluidized beds are involved often require heat transfer. Transfer to or from a fluidized bed can be accomplished by using the fluidizing air, the column wall, or an internal surface as the transferring medium. Heat can also be introduced to the bed by in-bed combustion of some material and the fluidizing air. This study was concerned with the use of internal heat transfer tubes.

An internal heat transfer surface usually consists of a bundle of tubes. As in conventional shell and tube exchangers, design is important. Both fluidized-bed and conventional heat exchangers benefit by the use of finned tubes. In heat exchangers

using fluidization the effect is mainly one of increased surface, whereas in the regular exchangers they are used as turbulence promoters as well.

In deciding on the best design of a multi-tube heat exchange bundle, three main factors must be considered: (1) the cost of construction and mounting in the fluidizing column, (2) pumping costs, and (3) the amount of surface area and heat transfer present with a particular design. Since most fluidized beds are in vertical cylinders, a vertical bundle is easier to mount in a vessel than one which is horizontal; however, this advantage has to be weighed against a possible decrease in heat transfer coefficients for tubes in the vertical position. If finned tubes are used, the effect on bundle fabrication and the effect on heat transfer coefficients will also be factors to consider.

It seems, therefore, that some knowledge about heat transfer coefficients obtained from tubes oriented at different angles would be helpful in deciding on a particular design for an in-bed heat exchanger. The objective of this study was to determine the effect of tube orientation on the heat transfer coefficients obtained from bare and finned tubes in a fluidized bed.

Studies have been made by other experimenters on heat transfer coefficients of bare tubes in fluidized beds; this is the first

investigation, however, which includes several orientations other than the horizontal and vertical positions. In addition to a bare tube, a tube with discontinuous fins was studied at various angles. A comparison of the author's experimental data with results of correlations of other investigators is presented in this dissertation.

THEORY AND LITERATURE SURVEY

Proposed Models for Fluidized Bed Heat Transfer

Various theories have been proposed by investigators for the mechanism of surface-to-bed heat transfer in a fluidized bed. All of them try to explain the fact that heat transfer with fluidization is greater than with one-phase flow. These theories can be classified into three main categories based on the mode of heat transfer. These models are: (1) the film theory, (2) the particle theory, and (3) a combination of both film and particle theories.

In the film models for heat transfer in a fluidized bed, the proposers regard the laminar layer existing at the surface as the main resistance to transfer. Leva et al (8), Levenspiel and Walton (9), and Dow and Jakob (3) explain increased heat transfer in a fluidized bed by the scrubbing action of the particles. This scouring at the surface is believed to destroy or decrease the thickness of the film which would allow for greater transfer to the surroundings. This model accounts for the characteristic maximum in the heat transfer coefficient as the flow rate is increased; increased velocity increases the scrubbing action but also decreases the concentration of particles which eventually causes a decrease in heat transfer.

The particle mode of heat transfer has been proposed by Mickley and Fairbanks (10), Ziegler, Koppel, and Brazelton (22), and Botterill and Williams (2). In these models, the particles themselves are considered to be heat transfer agents and the main factors in transferring heat to the bed. It is believed that particles from the bed are heated at the hot surface and then return to the bed where they dissipate the heat. Mickley and Fairbanks examined the situation by considering packets of particle emulsions; the controlling factor for heat transfer was thought to be the unsteady-state transfer from the wall to the packets by conduction. Botterill and Williams examined the conduction into the contacting particles and the fluid in the emulsion packet separately. Ziegler's model viewed a particle as a heat sink moving from the bed into the hot layer of fluid near the surface where it is heated by convection and then returns to the bed where it gives off its heat.

Van Heerden (17) took into account both film heat transfer and particle transfer in his model. He was able to predict values of heat transfer coefficients for transfer surfaces of different lengths and verify them experimentally. The model, however, considers a packet moving along the outer wall of a column and therefore would not be applicable to an immersed surface where the fluidization is not a steady downward movement of particles. The

other models were also developed from some vessel wall studies but are more applicable to immersed surfaces because the particles were assumed to be moving to and from the surface.

Of the proposed modes of surface-to-bed heat transfer, the particle model is probably the most correct. Evidence for this statement was obtained by experiments by Ziegler and Brazelton (21) and Shirai et al (15). They studied heat and mass transfer coefficients simultaneously in both one-phase flow and in a fluidized bed. If the film were the major resistance, the mass transfer coefficient would increase along with the heat transfer coefficient because of a decrease in film thickness. However, it was found that fluidized bed mass transfer coefficients were only slightly higher than coefficients in one-phase flow. Heat transfer coefficients increased 10 to 20 times (21). The experimenters concluded that most of the heat was transferred by the particle mode. Ziegler et al estimated 80 to 95% of transfer was accomplished by the particles; Shirai et al estimated approximately 88%. Ziegler and his co-workers predicted that the heat transfer coefficient is nearly independent of the thermal conductivity of the solid particles. This fact indicates that only the surface of a particle is heated and therefore it remains at the surface only a short time.

The model of Ziegler, Koppel, and Brazelton was used as a basis for correlating the experimental data of this investigation. The development of correlations is presented in a subsequent section of this dissertation.

Experimental Studies of Fluidized Bed Heat Transfer

Many variables must be considered when heat transfer in a fluidized bed is studied because of the complex nature of the system. These parameters are listed by Kunii and Levenspiel (6):

1. Properties of the gas:
   density, viscosity, specific heat
   thermal conductivity
2. Properties of the solid:
   diameter, density, sphericity, specific heat, thermal conductivity
3. Conditions at minimum fluidization:
   superficial velocity, voidage
4. Flow conditions:
   superficial velocity, void fraction
5. Geometric properties:
   bed diameter, diameter of immersed object, static bed height, length of heat exchange surface

Applying dimensional analysis to these parameter may give the following dimensionless groups (6):

$$\frac{hD_p}{k_g} = f\left(\frac{C_{pg}\mu}{k_g}, \frac{D_p \rho_g U_o}{\mu}, \frac{\rho_s}{\rho_g}, \frac{C_{ps}}{C_{pg}}, \frac{k_s}{k_g}, \frac{D_t}{D_p}, \right.$$

$$\left. \frac{L_f}{D_p}, \frac{L_h}{D_p}, \frac{L_h}{D_t}, \frac{L_f}{L_h}, \frac{U_o}{U_{mf}}, \epsilon, \epsilon_{mf} \right)$$

Because of the interrelationships between all these groups, they can be changed into many forms. This is the reason correlations given by different investigators often differ so much in form.

Surface-to-bed heat transfer in a fluidized bed has been studied both for vessel walls and for immersed objects. Since this study deals with internal tubes, only correlations for immersed surfaces will be presented here. Toomey and Johnstone (16) have shown that internal surfaces have higher coefficients except at high flow rates.

In this investigation, bare tubes were studied in vertical and horizontal positions. There are correlations in the literature for both positions; this permits verification of experimental accuracy.

Two relations are quite applicable to the horizontal tube situation. One is by Zenz and Othmer (20):

$$Nu = 14\ (G/G_{mf})^{.33}\ (Pr)^{.33}\ \left(\frac{D_t}{D_p}\right)^{.67}$$

Another correlation is by Vreedenberg (18):

$$Nu = 420\ (Pr)^{.3}\left(\frac{G\ D_t\ \mu}{D_p^3\ \rho_s \rho_g\ g}\right)^{.3}$$

For a vertical bare tube, a correlation by Wender and Cooper (19) is applicable:

$$h_b = \frac{.033\ C_R \left(\frac{D_p G}{\mu}\right)^{.23} \left(\frac{C_{ps}}{C_{pg}}\right)^{.8} \left(\frac{\rho_s}{\rho_g}\right)^{.66} k_g(1-\epsilon)}{D_p \left(\frac{k_g}{C_{pg}\ \rho_g}\right)^{.43}}$$

Correlations proposed by investigators are usually based on limited ranges of operating conditions, on limited geometry, and on limited ranges of bed and fluid properties. Therefore, it is important to try to use one which has been developed from conditions as close as possible to the situation under study.

EXPERIMENTAL APPARATUS

The equipment used in this investigation was constructed to permit the determination of surface-to-bed heat transfer coefficients and operating conditions in a fluidized bed. The major pieces of equipment were used previously by the Chemical Technology Division of Idaho Nuclear Corporation. Additions and modifications were made to these components so the system would be usable in the desired program.

The main components of the apparatus were the fluidizing column, a cyclone, measuring devices, heating elements, heat transfer tubes, and the bed material. Figures 1 and 2 are photographs of the experimental set-up and the tubes studied.

The fluidizing vessel used for experimentation was a 12-in. diameter, clear plastic column approximately 8 ft. in height, (See Figures 1 and 3). The column was equipped with a cyclone for particle loss prevention and a baffle plate to reduce elutriation. The bed was supported by a reinforced, perforated steel grid which distributed the fluidizing air in a nearly uniform manner. The column had a drain pipe and valve for removing the particles. A hole was bored in the column 25 in. above the grid to allow the use of a flexible funnel for filling. A metal bottom was used on the high pressure side of the grid to prevent rupture. The bottom was

removable to allow for changing the angle of the tubes being studied. Holes were drilled at various locations in the side of the vessel for electrical and thermocouple wire penetration.

Air flow into the vessel was measured by two rotometers; one was used for flow rates less than 13.5 SCFM and the other for higher flow rates up to 108 SCFM. Air from the source line was maintained at nearly 20 psig in the meters by using a pressure regulator. Detailed information on the rotometers and other devices is given in the Appendix.

The vertical pressure drop along the axis of the bed was measured by using three pressure taps at distances of 6, 13, and 25 in. from the grid. The taps were connected to two water manometers, as shown in Figure 3.

Iron-constantan thermocouples were used for both the bed and tube wall temperature measurement. The tube wall thermocouples were mounted as shown in Figure 4. The bed thermocouple was a sheathed couple passing through a fitting which allowed for radial movement across the bed. This was located 12 in. above the grid. A two-pen, continuous temperature recorder was used; the bed temperature range was 50 to 150°F, and the tube wall temperature range was 100 to 200°F.

Electrical heaters (See Figures 2 and 4) were used for heating the tubes. They were inserted snugly inside the tubes. The heaters were 1/2-in. in diameter and 9 in. long with a 6-3/4-in. heated length.

Electrical power to the heaters was controlled by a powerstat with a 120 volt electrical source. Wattage was determined by measuring current and voltage with a precision ammeter and a precision voltmeter.

The bare tube used was 5/8-in. stainless steel. The ends were insulated and a test section left exposed with five thermocouples attached, (See Figure 4). The finned tube was a 5/8-in. carbon steel tube with 3/4-in. discontinuous, spiral fins spaced at eight fins per inch. The fins were made of carbon steel and were 1/6-in. wide and .025-in. thick. The outside area per linear foot was 2.52 square feet. All but the test section of 6-7/8 in. was trimmed and insulated; five thermocouples were attached, (See Figure 4).

The experimental tubes were held firmly at any angle by a rectangular rack, (See Figure 5). The rack was equipped with clamps for holding the tubes and screws to permit it to be positioned and tightened in the 12-in. column.

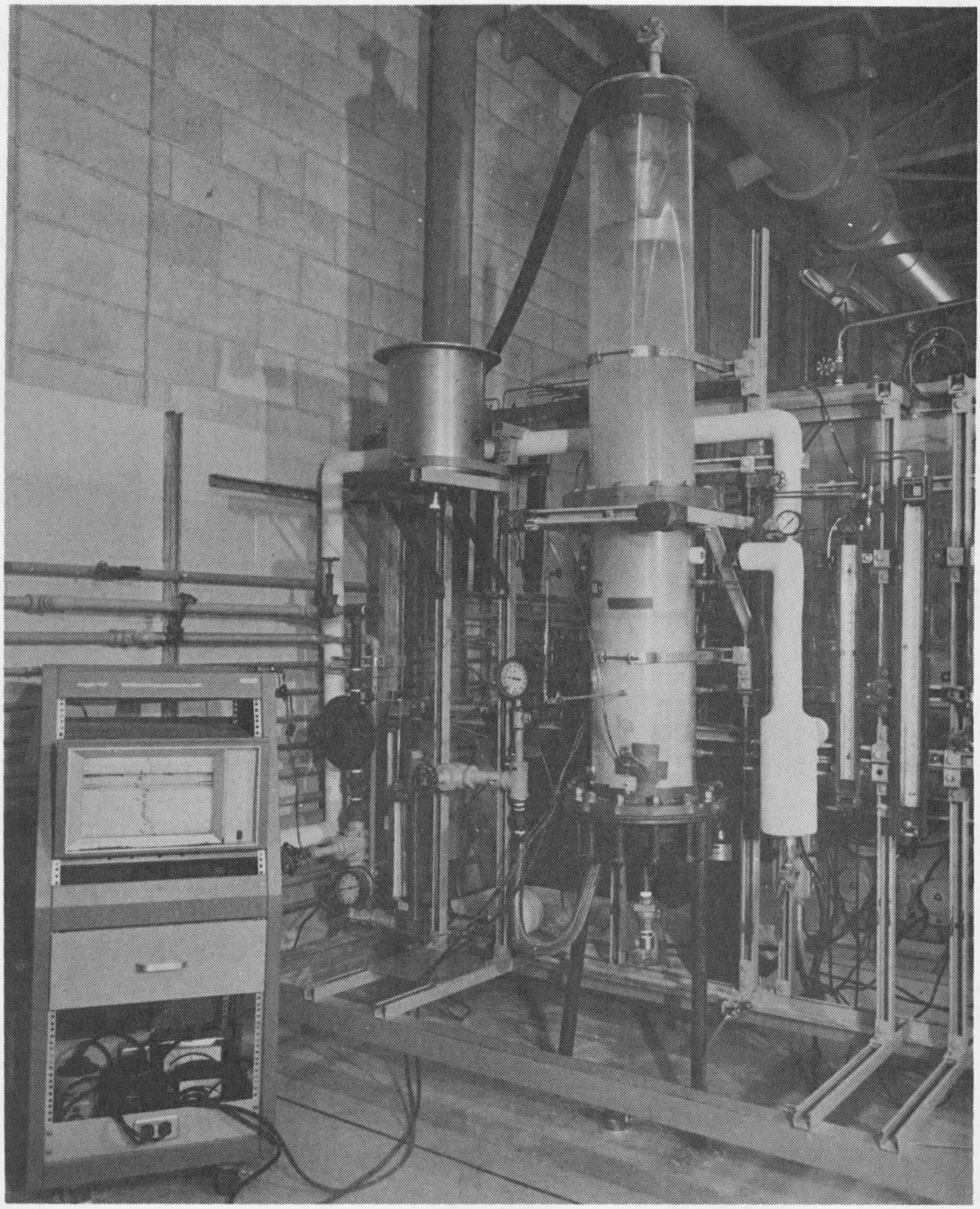


FIGURE 1. PHOTOGRAPH OF APPARATUS.

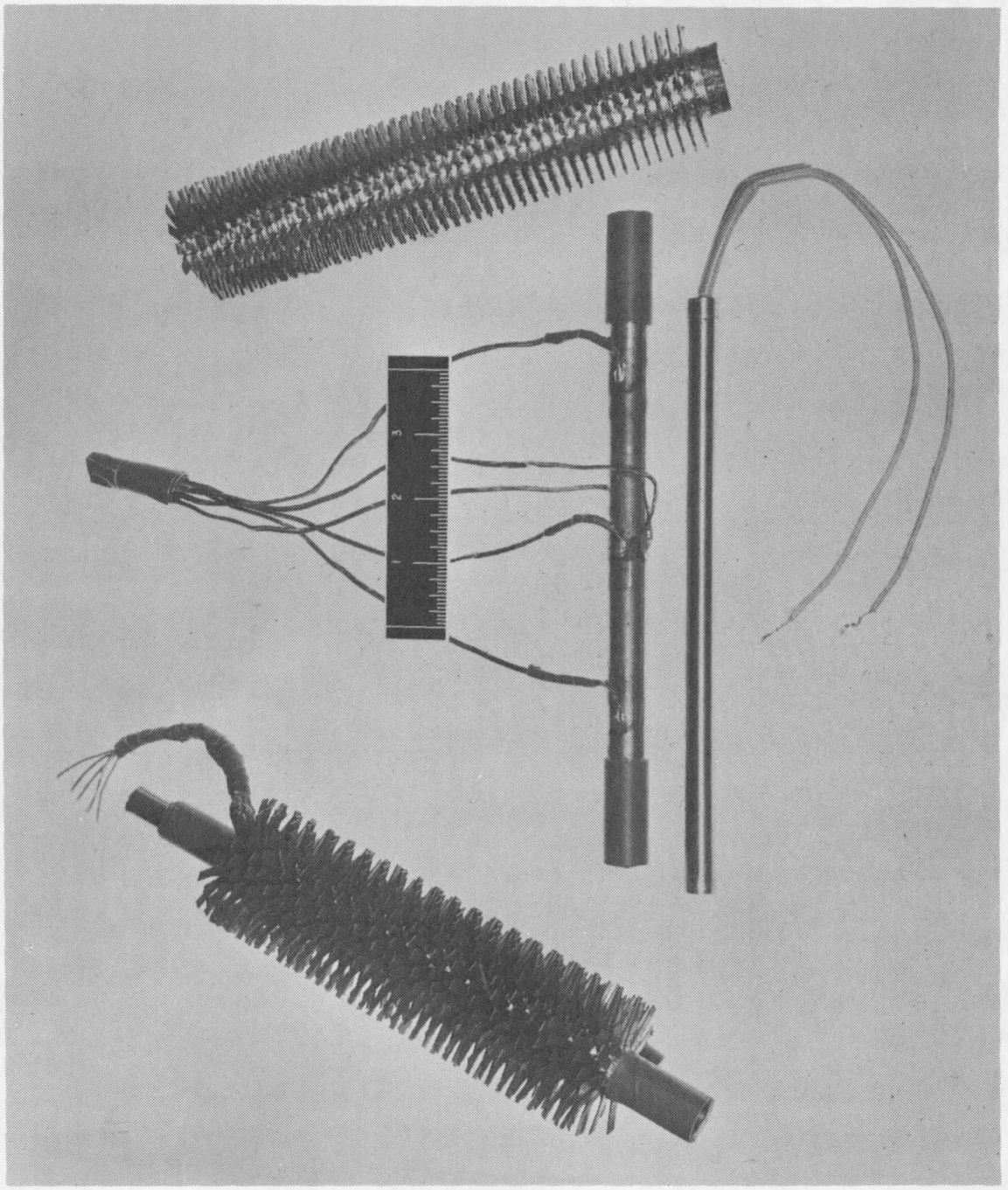


FIGURE 2. PHOTOGRAPH OF TUBES AND HEATER.

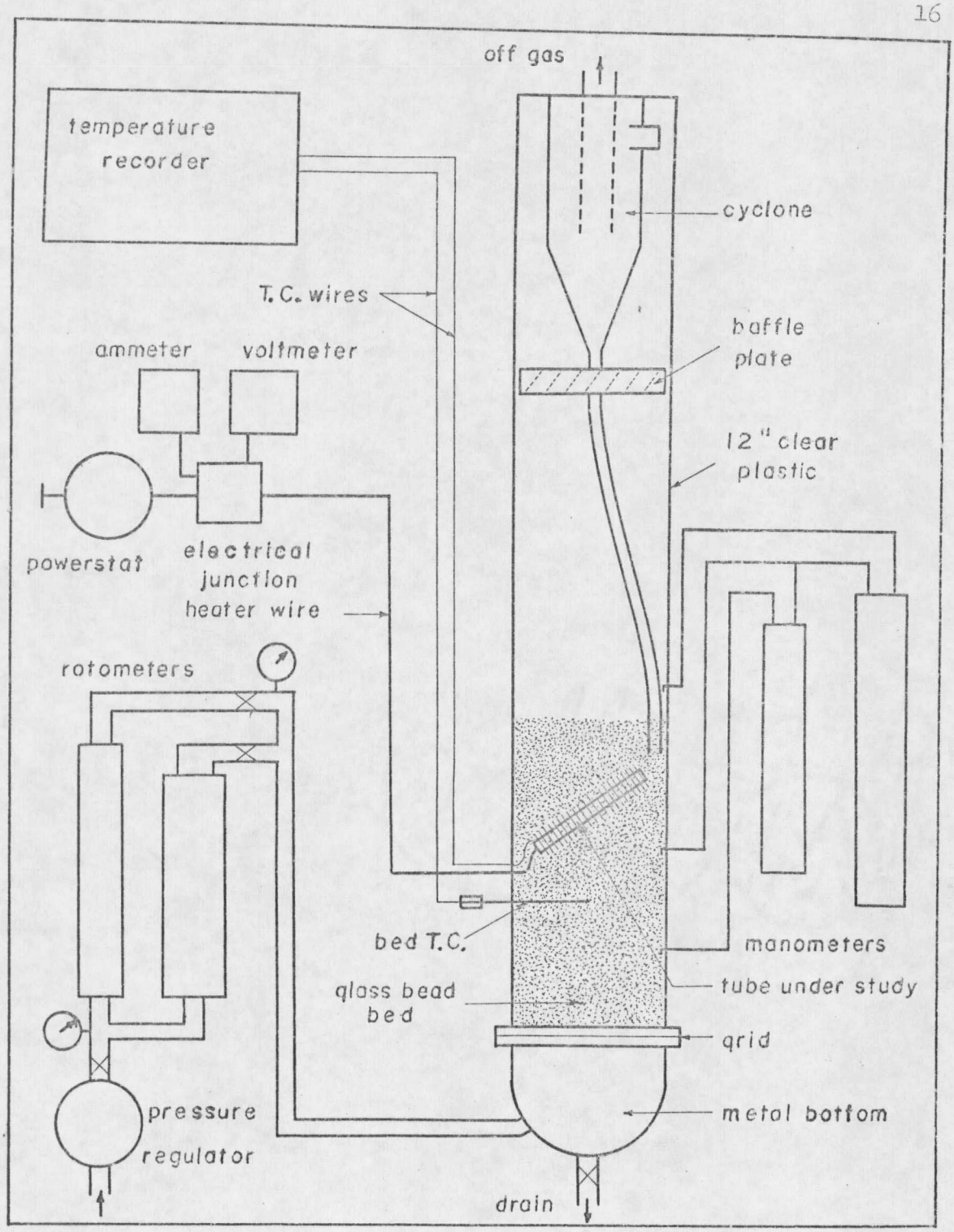
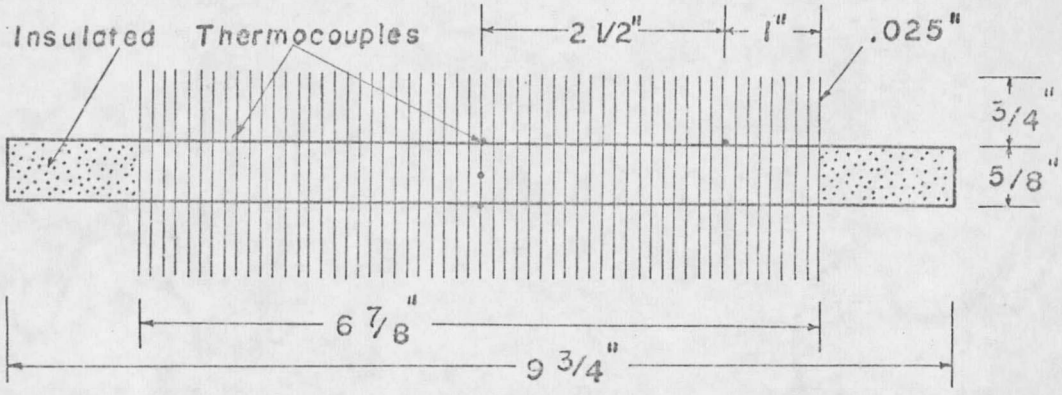
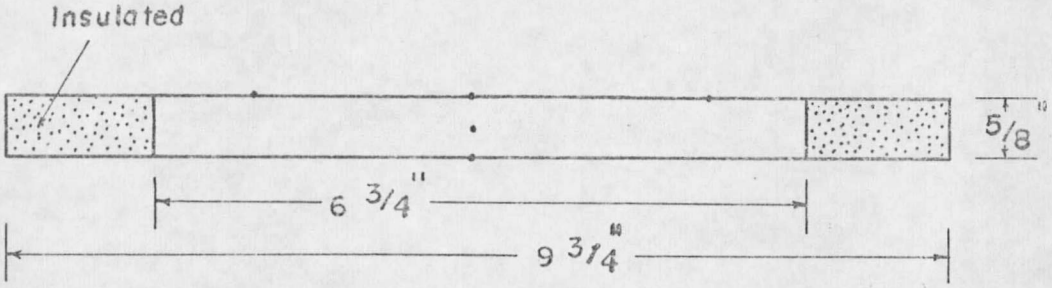


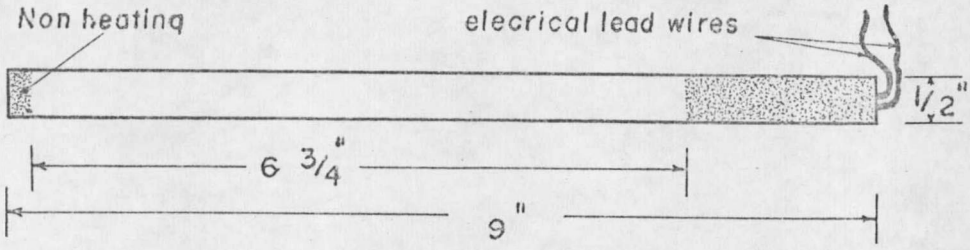
FIGURE 3. SKETCH OF APPARATUS.



Finned Tube



Bare Tube



Calrod Heater

FIGURE 4. DRAWING OF TUBES AND HEATER.

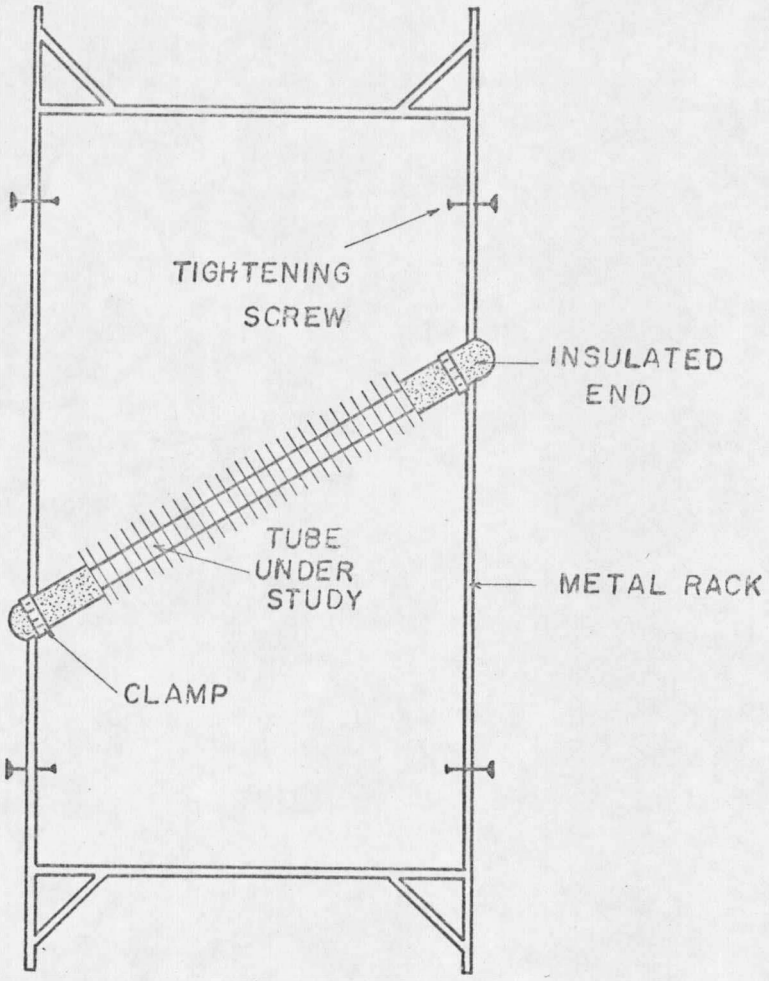


FIGURE 5. SKETCH OF RACK.

The bed material used was spherical glass beads. Three sizes were used: .0185, .0080, and .0045 in. in diameter. The beads were obtained from the Minnesota Mining and Manufacturing Company. Glass beads were chosen because of their uniform size and smooth, spherical shape.

A brief examination of the effect of fin thermal conductivity was made using a copper-clad finned tube somewhat similar to the carbon steel finned tube used in most of the experiment, (See Figure 2). The test section was the same length and the ends were insulated. The fins were spaced at six fins per inch and were 3/8-in. long and .030-in. thick. The tube diameter was one inch. A different electrical heater (3/4-in. diameter) was used to heat this tube.

EXPERIMENTAL PROGRAM

The determination of heat transfer coefficients for bare and finned tubes at various angles in a fluidized bed was the major objective of this study. An experimental program was designed to accomplish this objective and is presented here.

As discussed earlier, surface-to-bed heat transfer coefficients are affected by many variables. Generally speaking, these are gas properties, solid properties, conditions at minimum fluidization, flow conditions, and the geometry of the equipment. In this experiment, heat transfer coefficients were studied as functions of particle size, fluidizing velocity, tube angle, and tube type. All other variables were held constant, or as nearly constant as possible.

To determine the effect of these parameters, three particle sizes, five angles, various fluidizing air mass flow rates, and two types of tubes were used. The angles studied were 0°, 30°, 45°, 60°, and 90° with respect to the horizontal, (See Figure 6). The particle sizes and corresponding flow rates used with each rate are:

Fine Particles (.0045 in.):

65 to 270 $lb/hr\text{-}ft^2$ (6 rates)

3 to 13 times minimum fluidization mass flow rate, G_{mf}

Medium Particles (.0080 in.):

130 to 480 lb/hr-ft^2 (5 rates)

3 to 12 times G_{mf}

Large Particles (.0185 in.):

325 to 800 lb/hr-ft^2 (4 rates)

2 to 4.9 times G_{mf}

The upper limit on the mass flow rate was determined by flange leaks and particle loss through the cyclone.

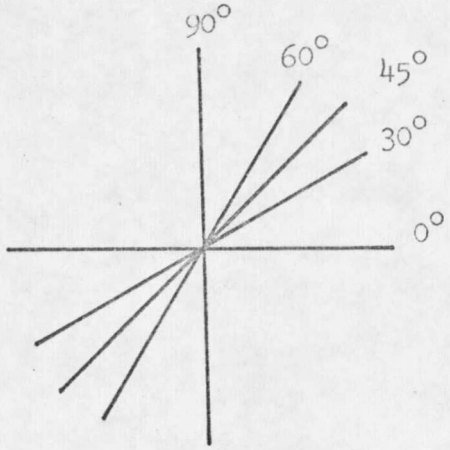


FIGURE 6. ANGLES INVESTIGATED.

The basic equation used in this study was that of convective heat transfer. (12):

$$q = h A(\Delta T)$$

The bed-wall heat transfer coefficient, h, can be found by measuring the other parameters in the equation. In this experiment, q was determined by measuring the power output of an electrical heater. The mean temperature difference was found by measuring tube wall and bed temperatures with thermocouples; five thermocouples were located on the tube and one in the bed. The surface area of the tubes was computed from measured dimensions.

To measure all the parameters, the following data were recorded for each run:

1. Pressure before rotometers
2. Pressure after rotometers and valve
3. Rotometer reading
4. Water level difference in first manometer
5. Water level difference in second manometer
6. Amperage in electrical circuit
7. Voltage across the electrical circuit
8. Temperature of the bed
9. Temperatures at five points on the transfer tube
10. Tube type
11. Tube angle
12. Particle size
13. Tube height (distance from grid)

The rotometer readings and pressure of the air entering the meters were used to calculate the flow rate. Manometer readings were used to determine the particle fraction, $(1-\epsilon)$, which was used in correlating the data.

A sample data sheet showing recorded data is included in the Appendix.

EXPERIMENTAL PROCEDURE

The following general procedure was used throughout the experiment:

1. The electrical heater was inserted in the finned tube. Care was taken to line up the heated portion of the heater with the uninsulated section of the tube. Ends and wires were taped to prevent particles from entering the tube.

2. The desired angle was set by arranging clamps at the correct trigonometric positions on the holding rack. Three thermocouples in a longitudinal row were always on the top of the tube.

3. The metal bottom of the column was removed to allow entry for the rack into the column where it was snugly fastened in position by using pressure screws. All wires were strung through the holes in the column and the bottom was bolted back on the vessel.

4. The bed thermocouple was centered at the axis of the vessel.

5. A static bed height of 22 in. was obtained by filling the column with the large size beads.

6. Four flow rates were used: 30, 45, 60, and 75% on the large rotometer. After thermal equilibrium was reached for each run, data were recorded.

7. The large size particles were drained and the column was filled with medium sized beads.

8. Five flow rates were used: 94% on the small rotometer, and 17.5, 23, 29, and 45% on the large rotometer. Data were recorded after thermal equilibrium was reached for each flow rate.

9. The medium size particles were replaced with the small size glass beads.

10. Six flow rates were used: 48, 72, and 96% on the small rotometer, and 15, 20, and 25% on the large rotometer; data were recorded as before.

11. The beads were drained and the rack removed. The bare tube was set at the next angle and steps 3-10 were repeated.

12. Steps 1-11 were repeated using the bare tube.

A determination of the minimum fluidization velocity was made for each particle size the first time each size was used.

All measuring instruments were calibrated by the instrumentation section of Idaho Nuclear Corporation.

A total of 154 scheduled runs were made. Fifteen additional runs were made as a recheck. Fifteen more runs (steps 1-10) were made with a copper-clad finned tube in the horizontal position giving a total of 184 experimental runs.

CALCULATIONS

In this experiment the heat transfer coefficient, h, was determined at different flow rates, tube angles, tube types, and particle sizes. It will be shown here how the different parameters involved in the study were calculated.

The heat transfer coefficient was calculated from the equation discussed in a previous section:

$$q = h A(\Delta T)$$

To determine h, the surface area of the tube, heat transfer rate, and mean temperature difference have to be obtained.

The surface area of the bare tube was calculated from dimensions and the finned tube area was determined from data given by the ESCOA Company. The heat transfer rate, q, was calculated by using the following relations:

Power (watts) = volts X amps

q (BTU/hr) = volts X amps X 3.4129 BTU/watt-hr

The average temperature was determined from the thermocouple readings. The method of obtaining the average temperature differed for finned and bare tubes. For the finned tube the thermocouples were placed on the test section as shown in Figure 4. This arrangement allowed measurement of point temperatures around

the tube as well as along the tube. By assuming that the temperature varied the same around the tube at the ends as it did in the middle, a total of twelve points can be used for determining an average. When all twelve points are considered, the average becomes

$$T_{av} = 1/12(4T_1 + 4T_3 + 6T_4 + 3T_5 - 5T_2),$$

where T_1 to T_5 are the point temperatures recorded by thermocouples. Development of this equation is given in the Appendix.

In the case of the bare tube, the method of averaging was less complex. The calrod heater used had a cool end, and temperatures could not be assumed to vary around the tube at the ends the same as at the middle. If this were assumed, the tube wall at the end could have been cooler than the bed temperature, which is impossible. Runs (#155-169) were made with a heater which did not have a cool end and averages using the finned tube method were determined. It was found that applying a simple 3-point average to the data obtained from the defective heater gave results which were in good agreement with the results obtained by applying the complex average to the good heater. Verification of this agreement (7% deviation) is given by data presented in the Appendix. Thus, the average temperature for the bare tube was obtained using the following average formula:

$$T_{av} = 1/3(T_1 + T_2 + T_3).$$

The mean temperature difference for all cases was the average tube temperature minus the temperature of the bed,

$$(\Delta T)\,av = T_{av} - T_b.$$

The mass flow rate, G, was determined from the rotometer reading using the following equation:

$$G(SCFM) = (\%\text{ reading on meter}) X (SCFM \text{ at } 100\% \text{ reading}) X \sqrt{\frac{\text{pressure into meter + atmospheric pressure}}{\text{standard pressure}}}.$$

The flow rate can be expressed in $lb/hr\text{-}ft^2$ by multiplying the right side of the equation by a conversion factor calculated from the inside diameter of the column. Hence, the relations used for calculating air flow rates from the small and large rotometers were:

<u>For small rotometer</u>:

$$G = (\text{scale reading}) X (13.45) X \sqrt{\frac{P_1 + 12.5}{14.7}} X 6.848$$

<u>For the large rotometer</u>:

$$G = (\text{scale reading}) X (108.3) X \sqrt{\frac{P_1 + 12.5}{14.7}} X 6.848$$

The particle fraction, $(1-\epsilon)$, was calculated from the manometer readings using the following relation given by Leva (7) for dense phase fluidization:

$$\Delta p = L\,(1-\epsilon)(\rho_s - \rho_g)\ ,$$

where L is the distance between the pressure taps and ϵ is the void fraction. The pressure drop, Δp, was determined from the water level differences in the manometers:

$$\Delta p = (\text{density of water}) \times (\Delta \text{height})$$

The value of $(1-\epsilon)$ for each flow rate was found by averaging all the values of $(1-\epsilon)$ at that flow rate.

Minimum fluidization velocity was calculated using Leva's relation (7):

$$G_{mf} = \frac{688\ D_p^{1.82}\left[\rho_g(\rho_s - \rho_g)\right]^{.94}}{\mu^{.88}}$$

Particle Nusselt numbers were obtained from experimental data by using the definition of Nu:

$$Nu = h\,D_p/k_g$$

Heat transfer coefficients and Nusselt numbers were calculated from the correlations presented heretofore, and from the

author's proposed correlations.

Calculations were made using a desk calculator and a digital computer.

DEVELOPMENT OF CORRELATIONS

Correlations for predicting Nusselt numbers were developed from data for both bare and finned tubes. They will be presented in this section.

The basis for both correlations is the model proposed by Ziegler, Koppel, and Brazelton (22):

$$Nu = \frac{7.2}{\left[1 + \frac{6\, k_g\, \bar{t}}{\rho_s\, C_{ps}\, D_p^2}\right]^2}$$

From studies made by Mickley (11) and Nöe (13), Gampson (4) and Genetti (5) concluded that the heat transfer coefficients of bare tubes were proportional to $(1-\epsilon)$ raised to approximately the 1/2 power.

Since the effect of tube angle, flow rate, and particle size were studied in this investigation, these were the main parameters used in correlating data. The mass flow rate was represented by the particle Reynolds number. The particle fraction was calculated and also included in the correlation.

Using the general form of Ziegler's model plus the results of Mickley et al, Nöe's, and Genetti's studies, the following general form was chosen for correlating the data obtained in this experiment:

$$Nu = \frac{K\,(1-\epsilon)^{1/2}}{\left[1 + C\,Re^{a}\left(\frac{D_p}{.008}\right)^{b}\right]^{2}}$$

where K is a constant, D_p is expressed in inches, and C is a function of tube angle.

Bare Tube

The dimensionless group, $\left[C\,Re^{a}\left(\frac{D_p}{.008}\right)^{b}\right]$, was called F and is defined from the above equation:

$$F = \sqrt{\frac{K\,(1-\epsilon)^{1/2}}{Nu}} - 1$$

The constant K was given a value of 11.0 to keep the F's calculated from experimental data positive. In order to determine the value of a, the exponent on particle Reynolds number, these values of F were plotted versus Reynolds number on log-log graph paper, (See Figure 7). Values of F were obtained for each tube angle and for each mass flow rate for the two smallest bed particle sizes. A straight line on this plot has the equation $F = C\,Re^{a}$, where a is the slope of the line. From Figure 7, the average slope was found to be about -.24. Thus, the exponent on Re is -.24.

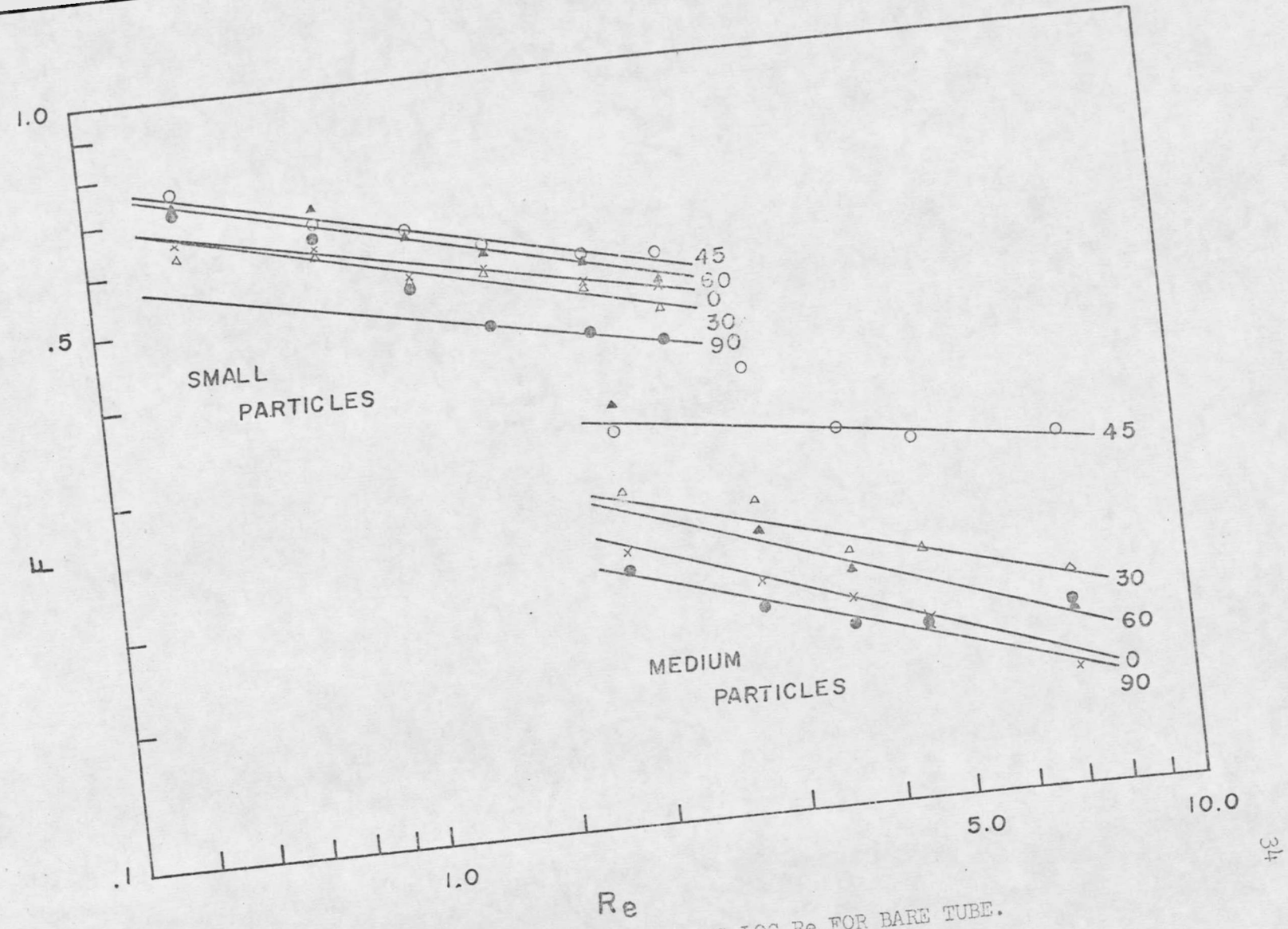


FIGURE 7. PLOT OF LOG F VERSUS LOG Re FOR BARE TUBE.

The exponent on the particle diameter divided by .008 in. was determined by a plotting method described below. From the dimensionless group F,

$$F = C\,Re^{a}\left(\frac{D_p}{.008}\right)^{b} ,$$

the following relation is determined by dividing by Re^a and taking the common log of both sides:

$$\log\left(\frac{F}{Re^{a}}\right) = \log C + b \log\left(\frac{D_p}{.008}\right)$$

It can be seen that this is an equation of a straight line and b is the slope of the line on a plot of $\log \frac{F}{Re^a}$ versus $\log \frac{D_p}{.008}$. Figure 8 is such a plot with average values of F/Re^a of different flow rates being used. From this plot the average slope was found to be -1.23, the value given to b, the exponent on $\frac{D_p}{.008}$.

From the above equation it is evident that when $\frac{D_p}{.008}$ is equal to one, $C = F/Re^a$. Hence, C can be expressed as a function of tube angle by plotting the values of F/Re^a at $\frac{D_p}{.008} = 1$ on Figure 8 for each angle versus that angle, (See Figure 9). The equation of the line in Figure 9 was found by trial and error. A least squares analysis of the third order was tried, but the re-

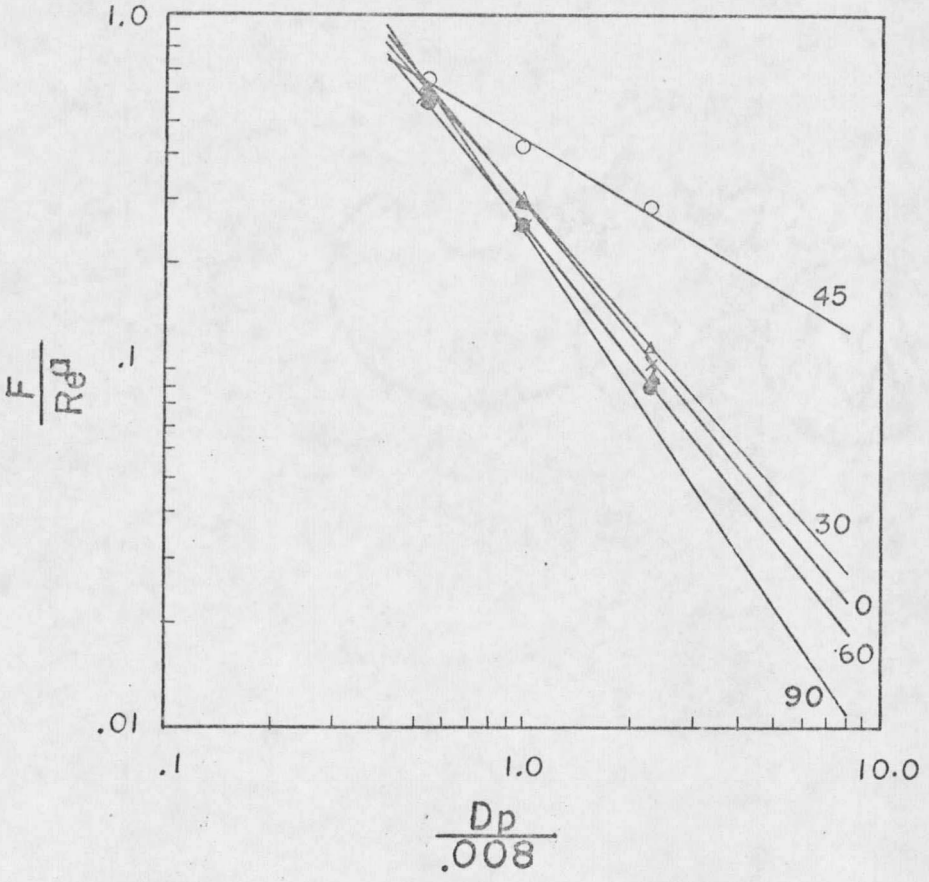


FIGURE 8. PLOT OF LOG $\left(\frac{F}{Re^a}\right)$ VERSUS LOG $\left(\frac{D_p}{.008}\right)$ FOR BARE TUBE.

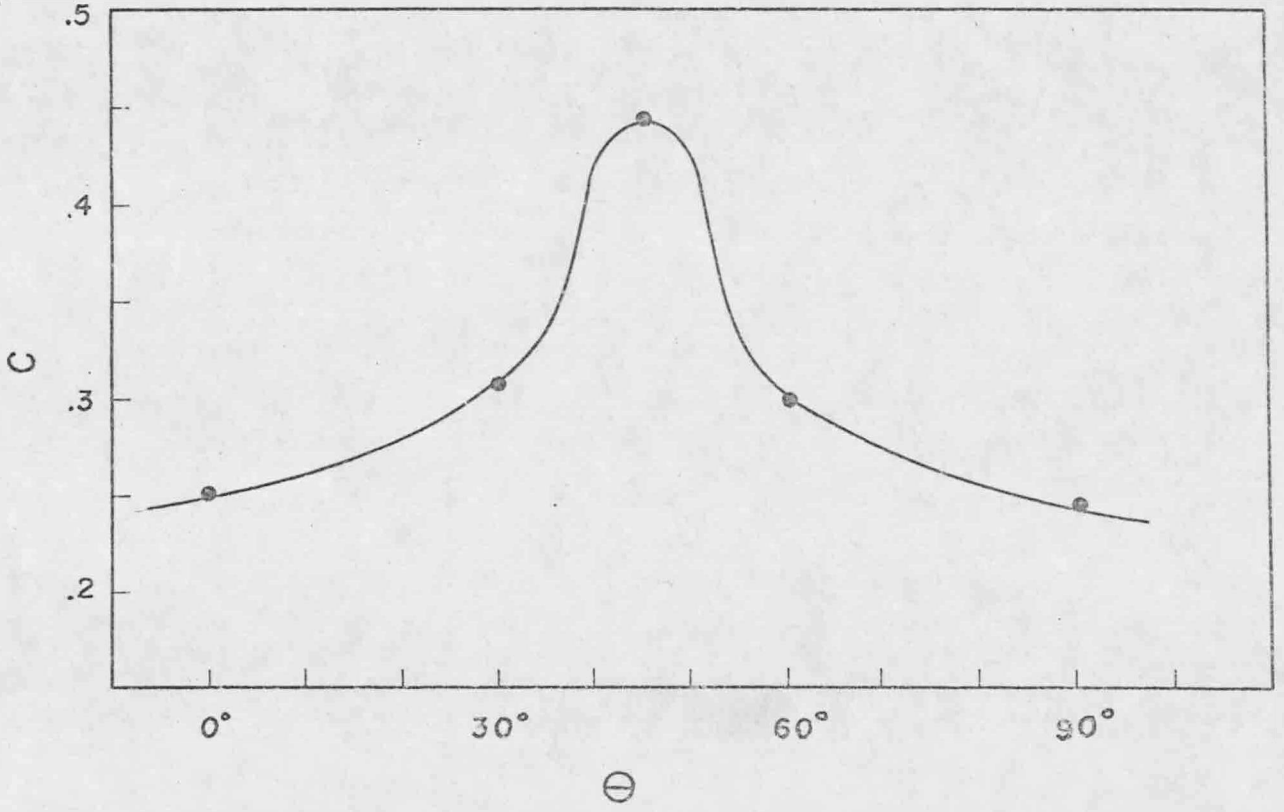


FIGURE 9. PLOT OF C VERSUS ANGLE FOR BARE TUBE.

sult was unsatisfactory. The equation for C was found to be

$$C = .44 - \frac{.20\ (\theta-45)^2}{(\theta-45)^2 + 120}$$

Therefore, the final relation for F is

$$F = \left(.44 - \frac{.20\ (\theta-45)^2}{(\theta-45)^2 + 120}\right) Re^{-.24} \left(\frac{D_p}{.008}\right)^{-1.23}$$

and the resulting final correlation of the data for the bare tube under the conditions investigated in this experiment is

$$Nu = \left[\frac{11\ (1-\epsilon)^{1/2}}{1 + \dfrac{.44 - \dfrac{.20\ (\theta-45)^2}{(\theta-45)^2 + 120}}{Re^{.24} \left(\dfrac{D_p}{.008}\right)^{1.23}}} \right]^2$$

where D_p is expressed in inches.

Finned Tube

Development of the correlation for the finned tube is much the same as that for the bare tube; however, experimental data is not used directly.

In the experiment, temperature differences were measured between the bed and the tube wall at the base of the fins. Since

temperature gradients existed along the fins, no overall average surface temperature was available for calculation. Heat transfer coefficients calculated with the measured temperature differences do not represent the effective temperature difference.

The rate of heat flow divided by the bed-to-wall temperature difference $q/\Delta T$, is available from experimental measurements. By deriving analytically an equation for bed-to-wall temperature difference as a function of the heat transfer coefficient, actual h's can be obtained.

By examining a differential element on a single fin of the tube, an equation for bed-to-wall temperature difference can be developed. Figure 10 illustrates an element of width δ, length ω, and thickness Δx. At the tip of the fins, $x = l$.

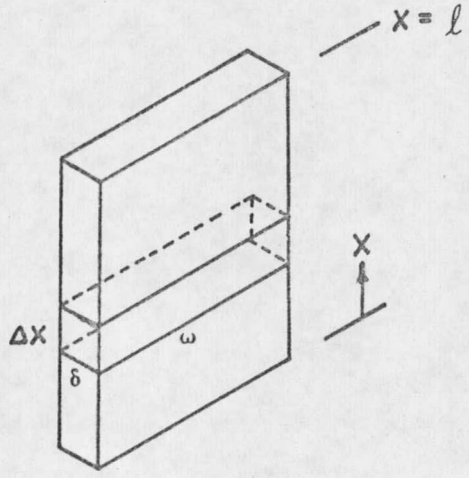


FIGURE 10. DIFFERENTIAL ELEMENT IN FIN.

In fluidization, radiation losses are small at temperatures less than 600°C (1) and can be neglected in this study. Thus, at steady-state conditions,

HEAT INPUT = HEAT OUTPUT.

Input to the element is by conduction only, whereas the output includes losses by both conduction and convection. By assuming that T is a function only of x and that k does not vary with temperature, the equation can be expressed as

$$-k\,\omega\,\delta\left.\frac{dT}{dx}\right|_{x} = -k\,\omega\,\delta\left.\frac{dT}{dx}\right|_{x+\Delta x} + h(2\Delta x\,\delta + 2\Delta x\omega)(T-T_b)$$

where $\omega\,\delta$ and $(2\,\Delta x\,\delta + 2\,\Delta\omega)$ are area terms, k is the thermal conductivity of the fin material, and h is the heat transfer coefficient which is assumed constant over the entire surface. By rearranging, dividing both sides of the equation by Δx, and taking the limit as Δx approaches zero, the equation becomes

$$\lim_{\Delta x \to 0} \frac{k\,\omega\,\delta\left.\frac{dT}{dx}\right|_{x+\Delta x} - k\,\omega\,\delta\left.\frac{dT}{dx}\right|_{x}}{\Delta x} = 2h(\delta+\omega)(T-T_b).$$

From the definition of a derivative, it can be expressed as

$$k\,\omega\,\delta\,\frac{d^2T}{dx^2} = 2h(\delta+\omega)(T-T_b).$$

The bed temperature is assumed to be constant at all points so it will not affect the value of a derivative; thus, $T-T_b$ can be sub-

stituted for T in the above derivative to give

$$\frac{d^2}{dx^2}(T-T_b) = \frac{2h(\delta+\omega)}{k\,\omega\,\delta}(T-T_b) = 0.$$

The general solution to this equation is

$$(T-T_b) = c_1 \sinh mx + c_2 \cosh mx$$

where

$$m = \sqrt{\frac{2h(\delta+\omega)}{k\,\omega\,\delta}}$$

Two boundary conditions needed for obtaining a particular solution are

1. at $x = 0$, $T = T_w$
2. at $x = l$, $h(T-T_b) = k\frac{d}{dx}(T-T_b)$

By applying the first boundary condition, sinh mx becomes zero and cosh mx becomes unity; thus,

$$c_2 = (T_w - T_b)$$

By applying the second boundary condition, the following is obtained:

$$-h/k\left[c_1 \sinh ml + (T_w-T_b)\cosh ml\right] = c_1 m \cosh ml + (T_w-T_b)\, m \sinh ml$$

The result of solving for c_1 from this equation is

$$c_1 = \frac{-(T_w-T_b)(h/k \cosh ml + m \sinh ml)}{(h/k \sinh ml + m \cosh ml)}$$

Thus, the final solution for finding the temperature difference on a single fin for any value of x and for any, h, k, δ, ω, T_w, or T_b is

$$(T-T_b) = \frac{-(T_w-T_b)(h/k \cosh ml + m \sinh ml) \sinh mx}{(h/k \sinh ml + m \cosh ml)} + \frac{(T_w-T_b) \cosh mx}{} \qquad \text{(equ. 1)}$$

The above equation can be used to obtain an equation for $q/(T_w-T_b)$ for the entire finned tube. This type of equation is needed to get actual heat transfer coefficients by knowing experimental values of $q/(T_w-T_b)$.

All of the heat given off by the entire tube surface can be expressed as

$$q_t = Nq_f + q_w \quad , \qquad \text{(equ. 2)}$$

where q_t is the total heat transfer rate, q_w is the rate of transfer from the wall, q_f is the rate from one fin, and N is the total number of fins on the tube. The heat flow rate from the wall of the tube is

$$q_w = hA_w(T_w-T_b).$$

Heat transferred from all of the fins can be expressed as the number of fins times the heat entering each fin at its base:

$$Nq_f = N\left[-kA_{bf} \frac{d}{dx} (T-T_b)\Big|_{x=0} \right],$$

where A_{bf} is the area of the base of one fin. The value for the derivative can be obtained from equation (1), and is expressed as

$$\frac{d}{dx} (T-T_b)\Big|_{x=0} = \frac{-(T_w-T_b)(h/k \cosh ml + m \sinh ml)}{(h/k \sinh ml + m \cosh ml)} m$$

By substituting the above values into equation (2) and dividing both sides by the temperature difference, the following relation is obtained:

$$\frac{q_t}{(T_w-T_b)} = mN\left[\frac{kA_{bf}(h/k \cosh ml + m \sinh ml)}{(h/k \sinh ml + m \cosh ml)} \right] + hA_w$$

which is the desired equation.

Using this equation, a plot of $q/(T_w-T_b)$ obtained from this study versus h was made using arbitrary values of h, (See Figure 11). From this plot, values of h for the finned tube can be obtained by using the values of $q/(T_w-T_b)$ available from experimental data. These coefficients describe the actual situation better than those based on the bed-to-wall temperature difference and were used for the correlation development that follows.

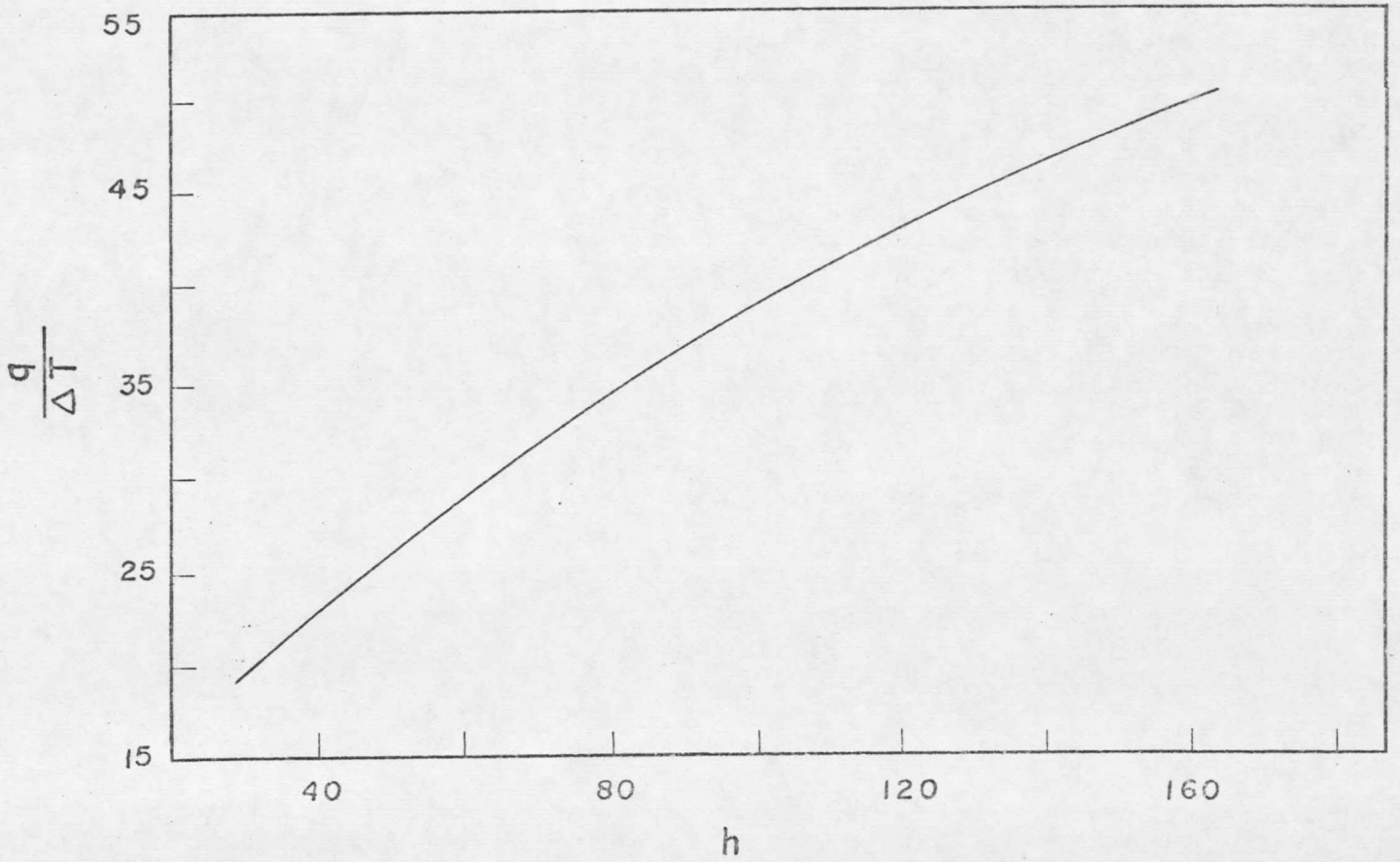


FIGURE 11. PLOT OF q/Δ T VERSUS h.

Using the same procedure for correlating finned tube data as for the bare tube data, the values of F were calculated and plotted versus particle Reynolds number on log-log paper. The slope of the dashed line in Figure 12 is -.51. This value was taken as a, the exponent of Re in the expression for F. The dashed line in Figure 12 follows the two smallest particle sizes more closely than the larger size because the heat transfer coefficients were influenced more by Reynolds number in these sizes.

As before, log $\frac{F}{Re^a}$ was plotted versus log $\frac{D_p}{.008}$, (See Figure 13), to determine b, the exponent on $\frac{D_p}{.008}$. Again, average values of $\frac{F}{Re^a}$ were used for each group of flow rates at a given angle and particle size. From this plot, the average slope was -.35, which is the value given to b. At this point the expression for F is partially complete:

$$F = CRe^{-.51}\left(\frac{D_p}{.008}\right)^{-.35}$$

As in the case for the bare tube, the value of C equals the value of log $\frac{F}{Re^a}$ at log $\frac{D_p}{.008}$ equal to one. These values were taken from Figure 13 and used to plot Figure 14, where C is represented as a function of tube angle. This curve could not be matched accurately enough with an equation to be used in a final correlation. Thus, C, a function of tube angle, must be obtained

from Figure 14. By substituting the expression derived for F into the basic correlation form, the following final correlation for the finned tube studied is obtained:

$$Nu = \frac{11\,(1-\epsilon)^{1/2}}{\left[\,1 + \dfrac{C}{Re^{.51}\left(\dfrac{D_p}{.008}\right)^{.35}}\,\right]^2}$$

where D_p is expressed in inches and C is found from Figure 14.

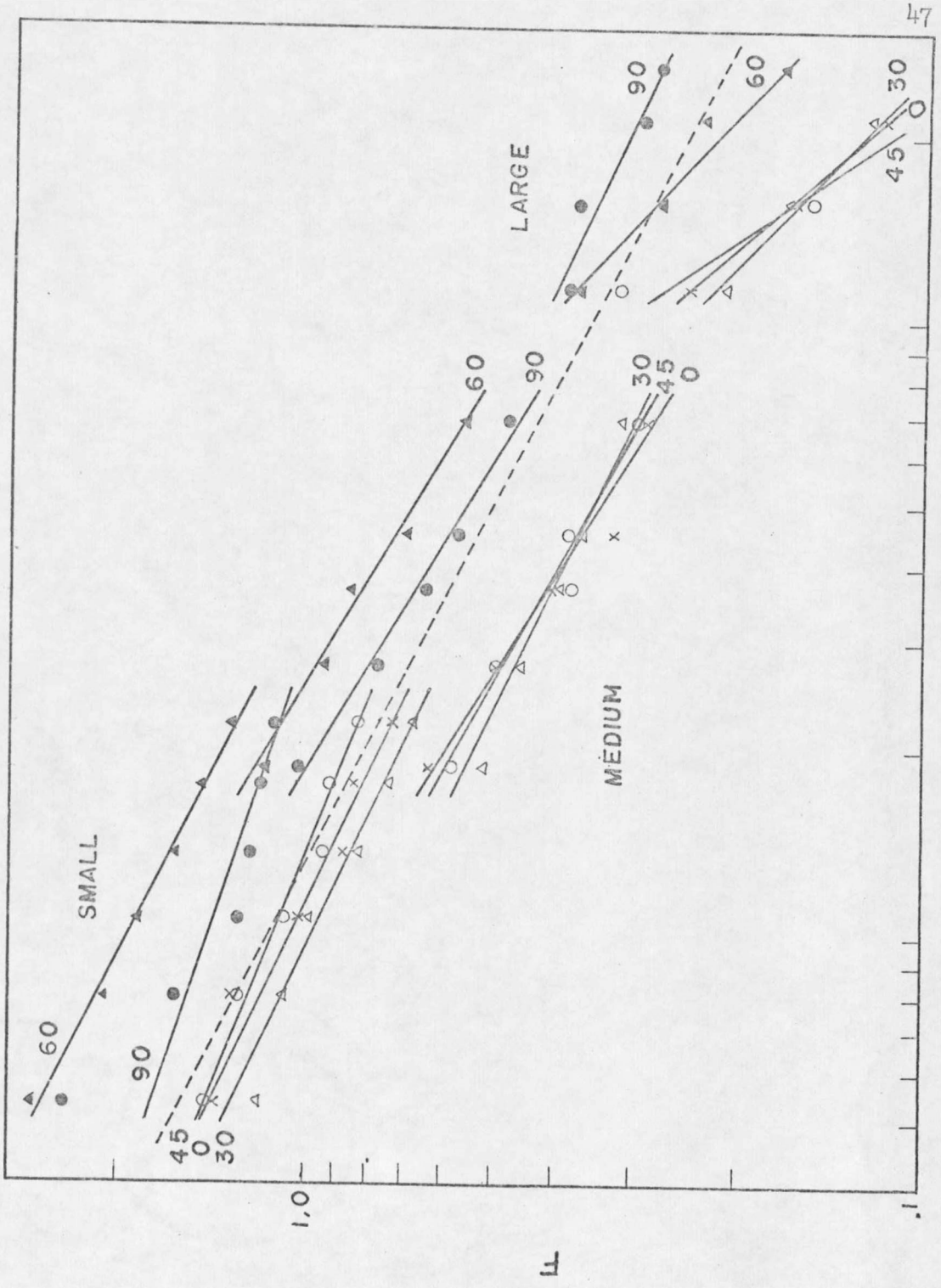


FIGURE 12. PLOT OF LOG F VERSUS LOG Re FOR FINNED TUBE.

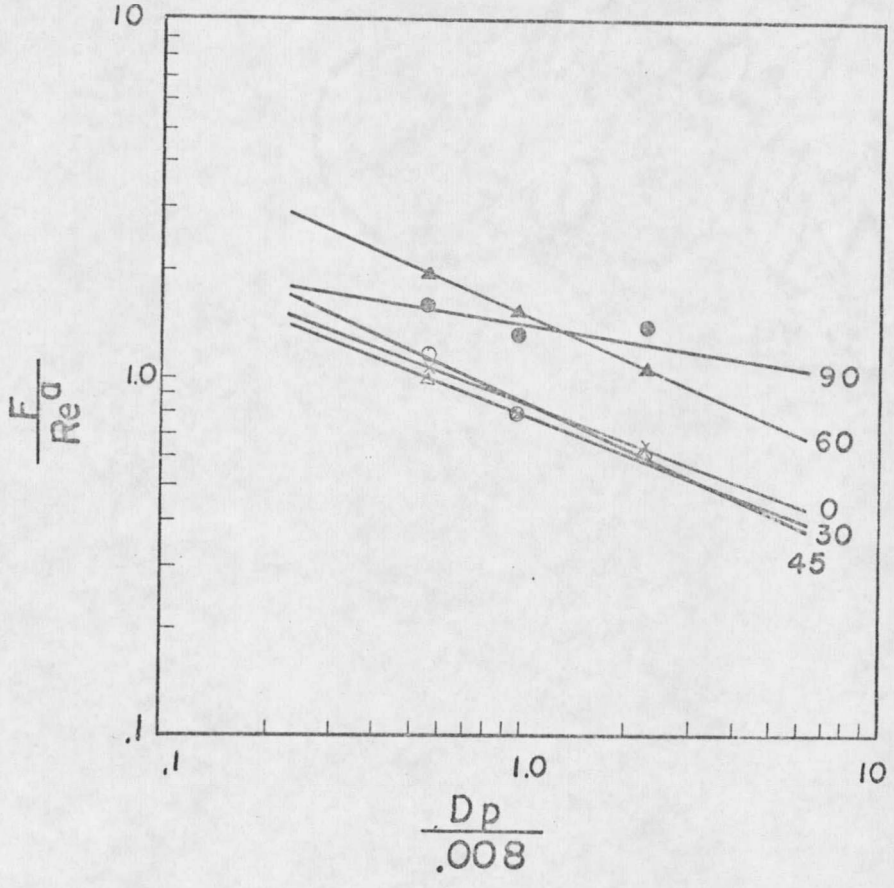


FIGURE 13. PLOT OF LOG $\frac{F}{Re^a}$ VERSUS LOG $\frac{D_p}{.008}$

FOR FINNED TUBE.

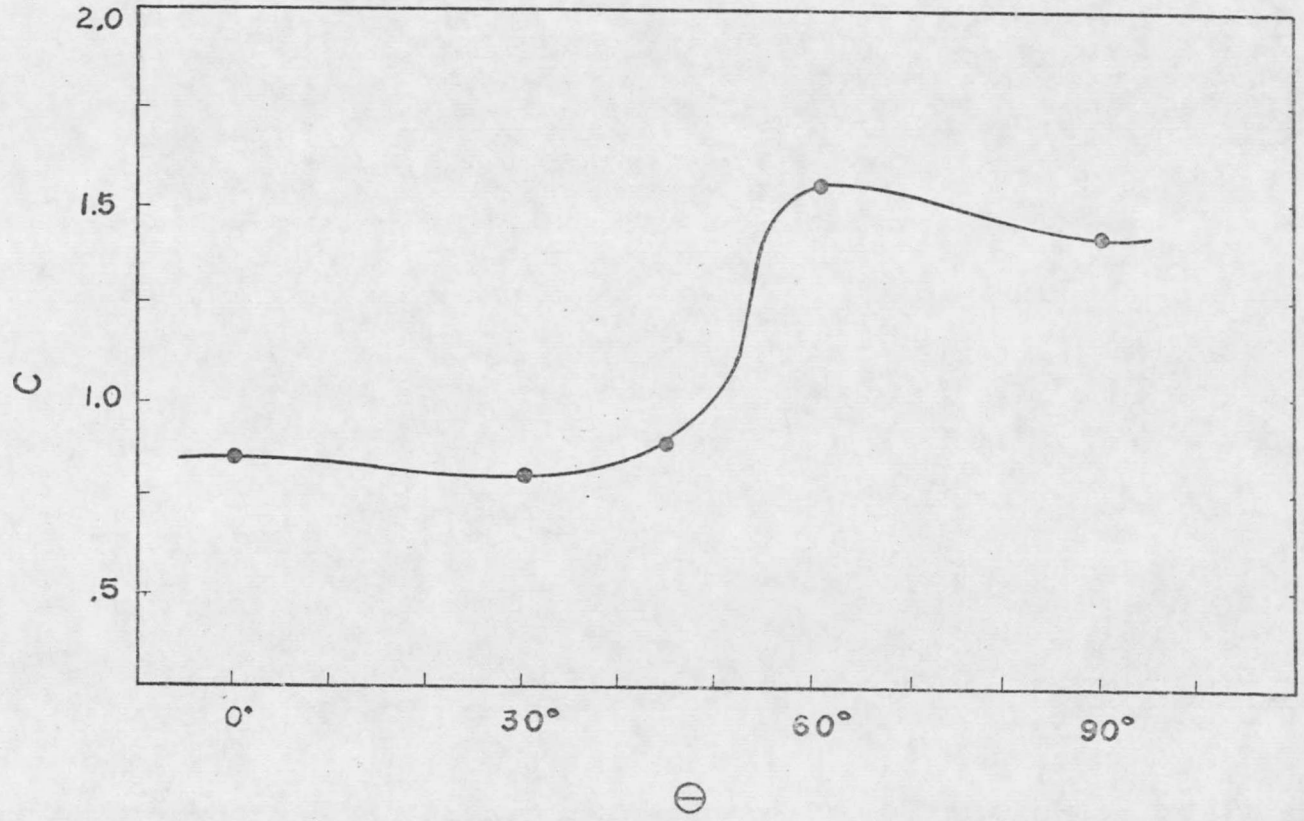


FIGURE 14. PLOT OF C VERSUS ANGLE FOR FINNED TUBE.

RESULTS AND CONCLUSIONS

Results and Discussion

One significant advantage of using a transparent vessel is that it allows direct observation of bed fluidization. The minimum fluidizing velocity -- the minimum gas flow rate needed to cause bed expansion -- was easily determined by observing bed characteristics. For each particle size, the minimum fluidizing velocity, G_{mf}, was determined by visual observation and also by Leva's correlation. A comparison of results is shown in Table I. Figure 15 indicates that the experimental values for G_{mf} were higher than those given by Leva's equation.

TABLE I

COMPARISON OF EXPERIMENTAL VALUES OF G_{mf} AND VALUES PREDICTED BY LEVA'S EQUATION

D_p (in.)	G_{mf} (Leva) (lb/hr-ft^2)	G_{mf} (Exp) (lb/hr-ft^2)	% Deviation
0.0045	11.6	20.5	76.7
0.0065	22.6	----	----
0.0080	33.0	41.1	24.5
0.0130	79.8	----	----
0.0185	152.0	164.0	7.9

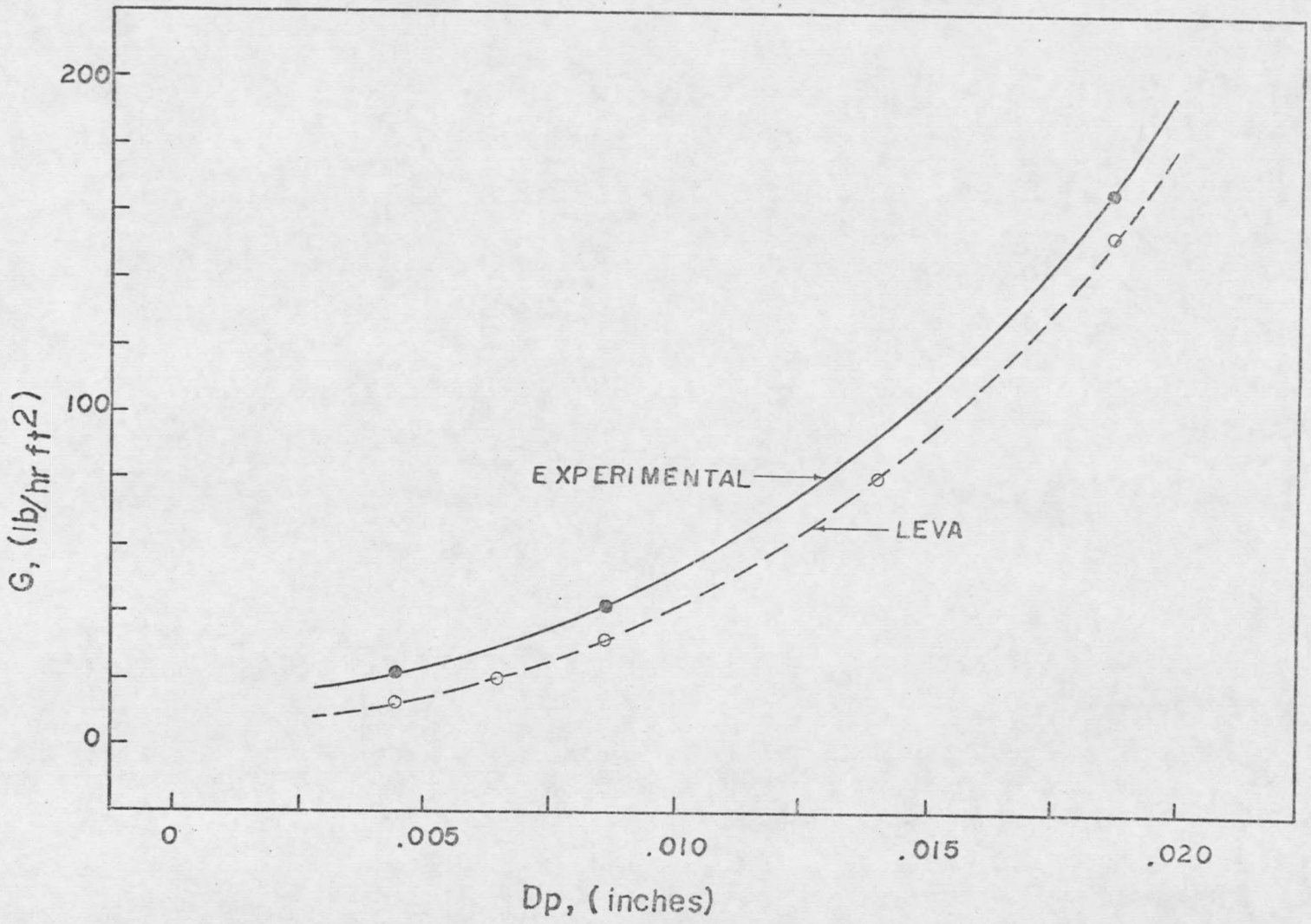


FIGURE 15. COMPARISON OF PREDICTED AND EXPERIMENTAL MINIMUM FLUIDIZATION VELOCITIES.

The main reason for the larger derivation at low flow rates is probably uneven distribution of air by the fluidizing grid since the air entered the bottom of the column at a slight angle. Also, the fact that the vessel was 12. in. in diameter makes it bigger than most of the columns used by other investigators determining minimum fluidizing gas flow rates. Because the values of G were small, a slight error in reading the rotometers results in a significant per cent deviation. It can be seen from Table I that agreement was good at the higher flow rates.

The results of examining the bare tube at the five angles described earlier are shown in Figure 16. The change in the heat transfer coefficient h_b with a change in flow rate is shown for each particle size and angle. Note that the abcissa scale is discontinuous to avoid crowding the data.

It is evident from Figure 16 that a minimum value for the coefficient is reached at 45° for each family of curves. This minimum was not expected and poses a difficult question as to why it exists. The results are probably due to the particle contact time -- the time a particle spends in the hot fluid layer -- which depends upon the fluidizing action around the immersed object. The explanation presented here is based on the probable movement of particles near the surface of the tube. It has been shown (22) that the

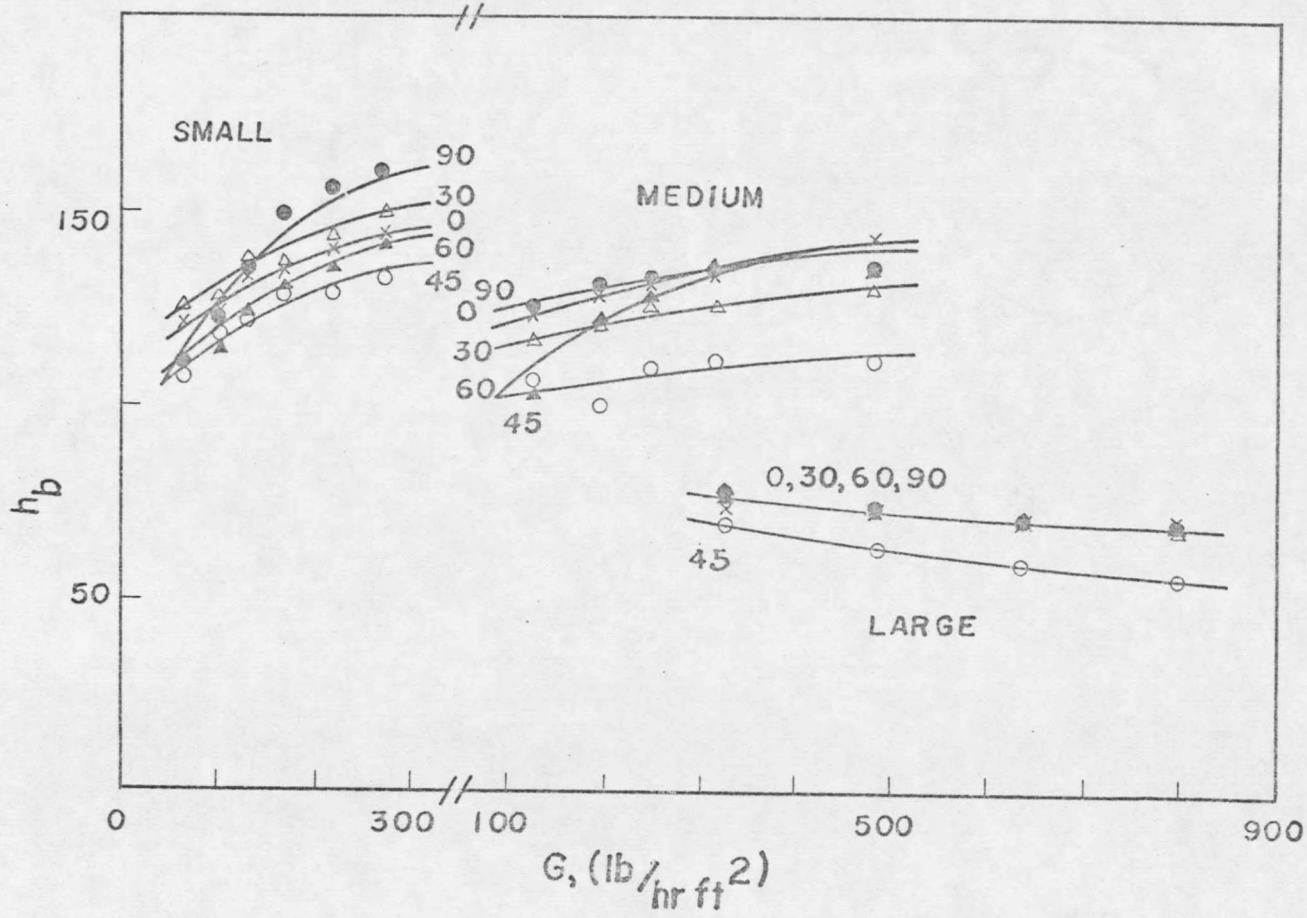


FIGURE 16. RESULTS OF BARE TUBE STUDY.

shorter the particle contact time, the higher the heat transfer coefficient will be.

If the tube is in the horizontal position, the particles are moving upward and around the circumference of the tube. This action produces a short contact time and good heat transfer. However, in this position a region of less vigorous particle movement exists at the top side of the tube giving longer contact times to the particles. This becomes a disadvantage to the horizontal position. With the tube in the vertical position, the contact time is longer due to the movement of particles along the tube, but there is no region of limited activity; thus, the tube performs similarly in these two positions. In the 45° position, the particle contact time is greater than in the other positions because both the effects which produce increased contact time are present. There is a sluggish region existing above the tube and the length of the surface along the flow of the particles is greater than that in the horizontal position. Because of these two contributing factors, the heat transfer rate is lowest in the 45° position.

Since bare tube correlations are available in the literature, some were used to check the validity of the results obtained in this investigation. If the results of the study on the horizontal and vertical positions are in agreement with those from the literature,

then it can be assumed that data obtained from studying the angles between these positions are also valid.

In the case of the horizontal bare tube, two relations are quite applicable. These are Zenz and Othmer (20) and by Vreedenberg (18) and were presented previously in this dissertation. Figure 17 shows a comparison of the experimental results with the results of these two correlations. It can be seen that the experimental agreement is quite good; as good as the agreement between the two correlations, (See Table II).

Figure 18 shows a comparison of the experimental results of the vertical bare tube and a correlation by Wender and Cooper (19). Again the agreement is reasonably good, (See Table II). Hence, the data from the 30°, 45°, and 60° positions should be quite reliable.

TABLE II

COMPARISON OF DATA FROM CORRELATIONS AND EXPERIMENT

Tube Position	Particle Size	Average Per cent Deviation		
		Zenz-Othmer	Vreedenberg	Wender-Cooper
Horizontal	Small	32.5	7.6	
	Medium	12.0	51.6	
	Large	34.0	40.1	
Vertical	Small			18.6
	Medium			55.2
	Large			43.1

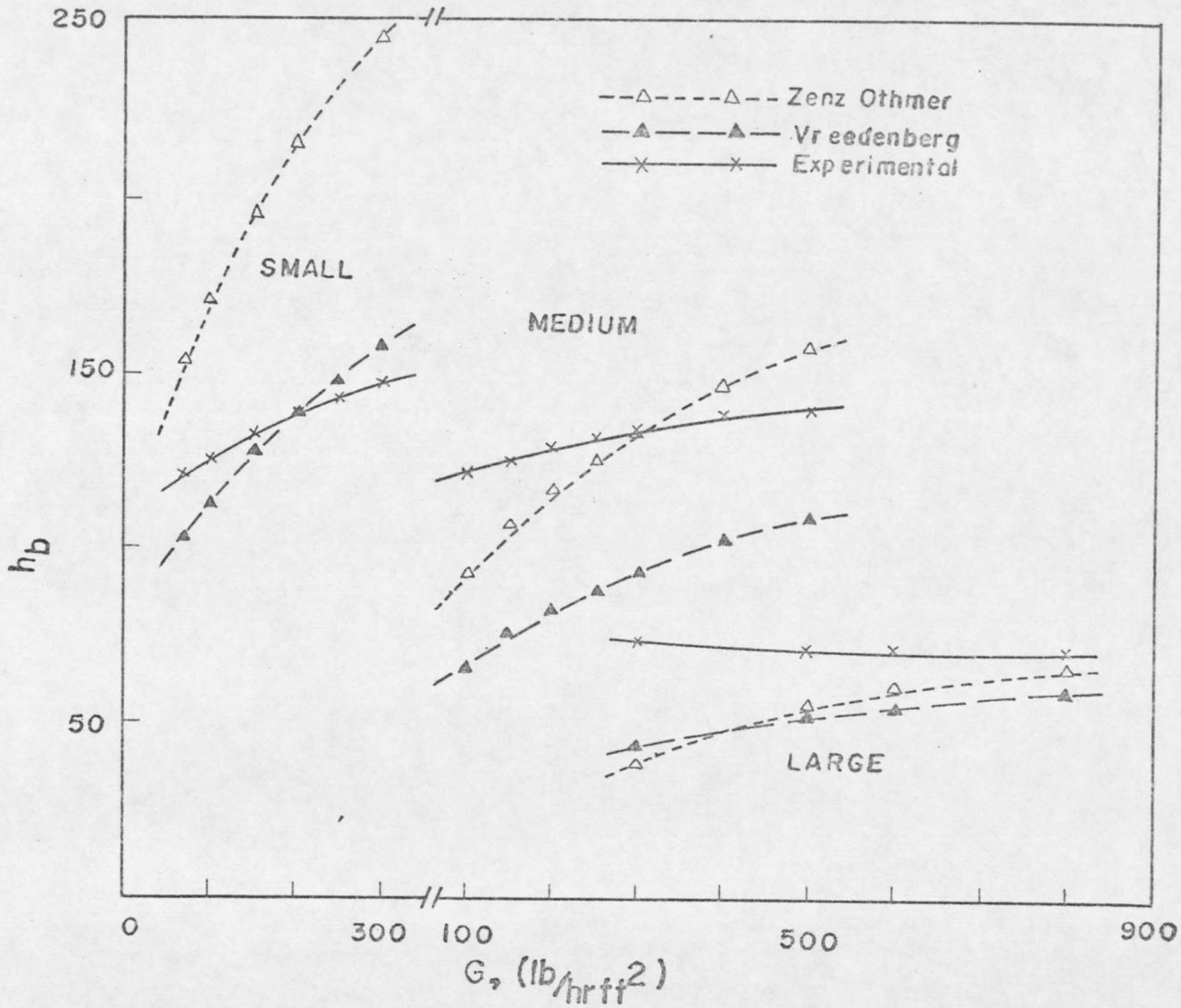


FIGURE 17. COMPARISON OF HORIZONTAL BARE TUBE COEFFICIENTS AND PREDICTED VALUES.

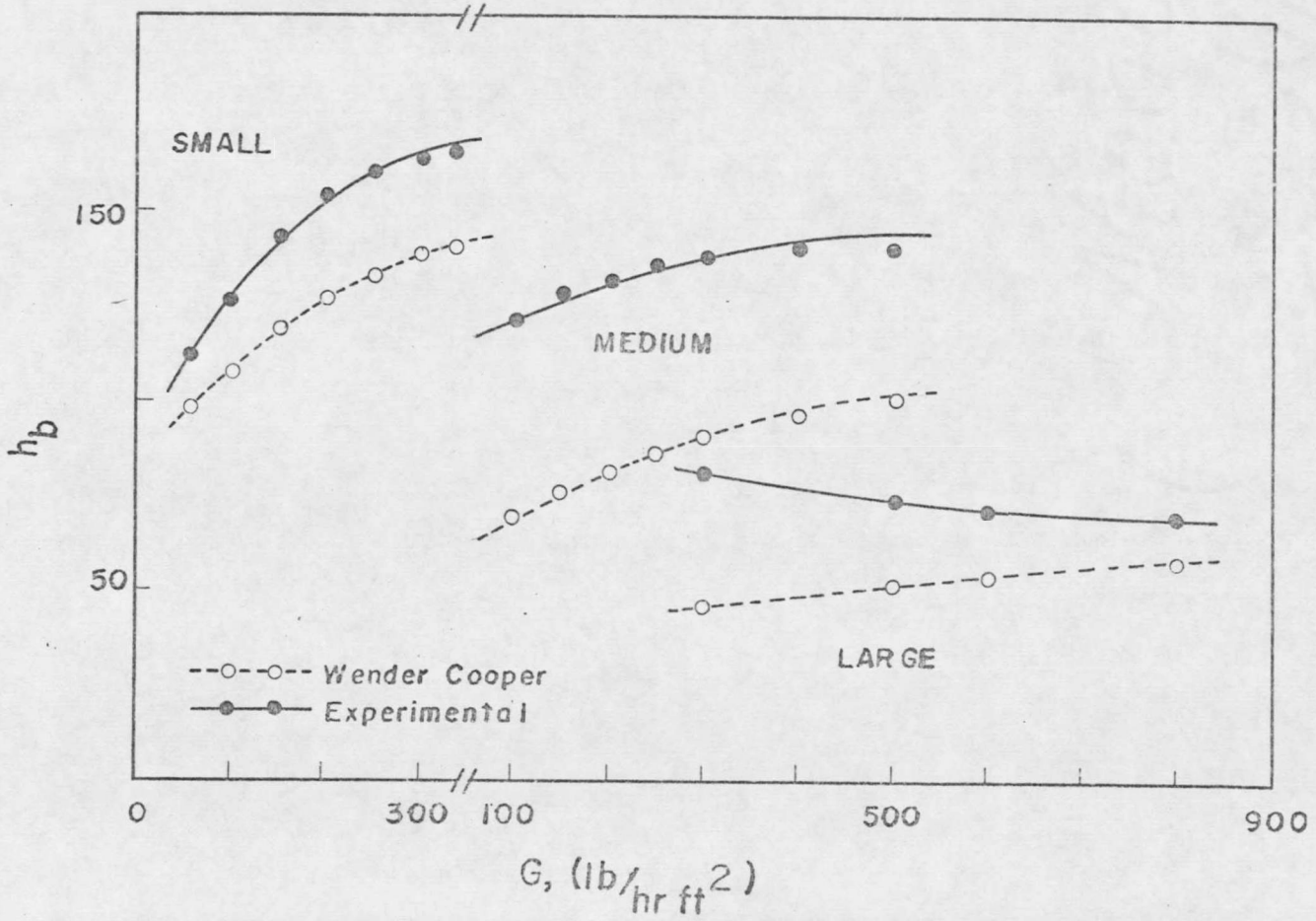


FIGURE 18. COMPARISON OF VERTICAL BARE TUBE COEFFICIENTS AND PREDICTED VALUES.

The results of the correlation developed by the author for the bare tube are compared to experimental results in Figures 19 and 20. Figure 19 is a plot of actual particle Nusselt numbers versus particle Nusselt numbers calculated using the correlation. The average deviation of the experimental values from the calculated values is 7 per cent. Figure 20 shows the values of experimental and calculated heat transfer coefficients.

The average effect of angle on the coefficient of the bare tube as predicted by the correlation is shown in Figure 21. The value of the coefficient is expressed as a per cent of the horizontal coefficient and is plotted versus angle for each particle size.

Before presenting the results from the finned tube study, a discussion on effectiveness factors will be presented. For design purposes, the following equation can be used for finned tube (14):

$$q = h_b \phi A_f (\Delta T)$$

where ϕ is the effectiveness factor. Since there is a temperature gradient in each fin, an equation of the form $q = h_{ff} A_f (\Delta T)$ cannot be used since no definite temperature difference would be known for the whole finned tube. The fin effectiveness factor is a fin efficiency term which enables the use of the bare tube coefficient, h_b. If fins had a uniform temperature all over equal to that at the

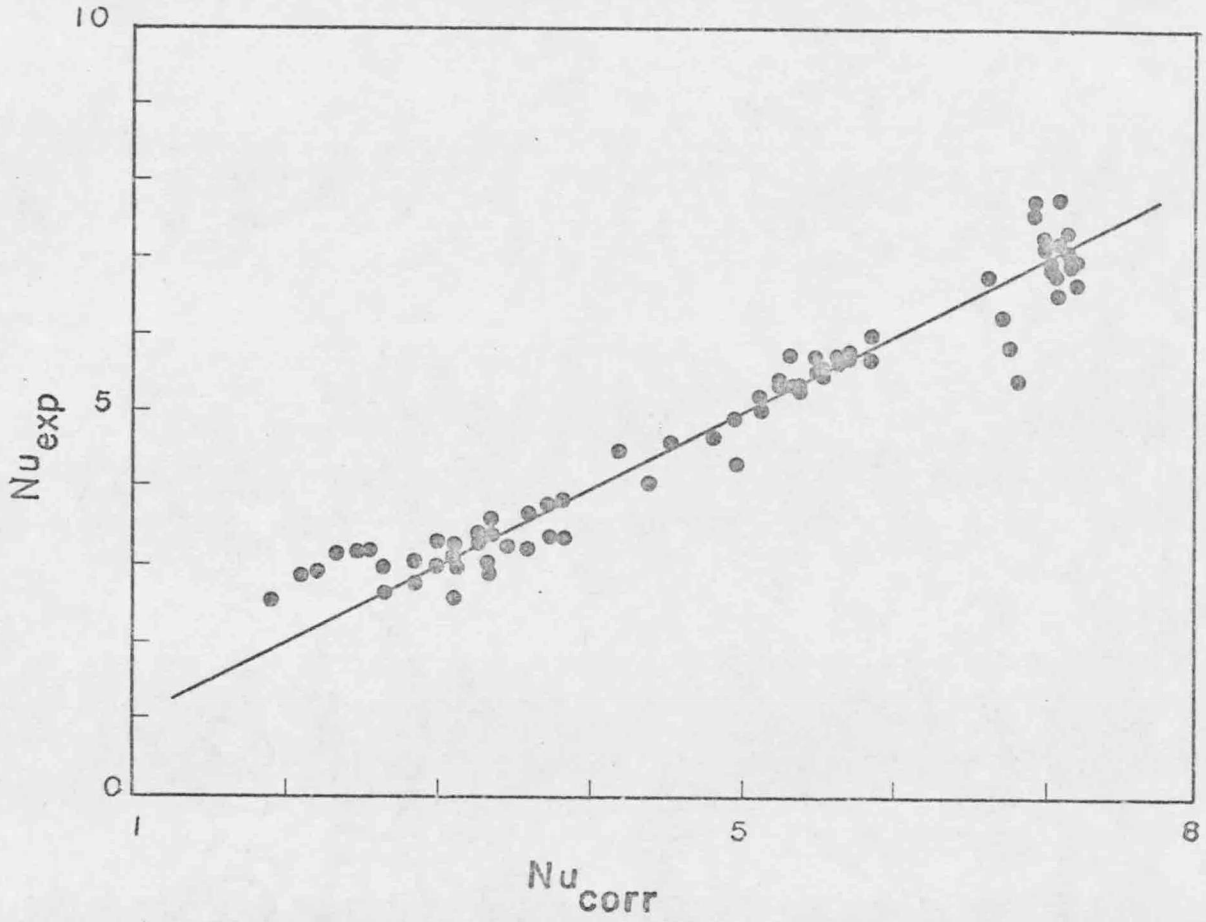


FIGURE 19. COMPARISON OF EXPERIMENTAL Nu's AND THE AUTHOR'S CORRELATION (BARE TUBE).

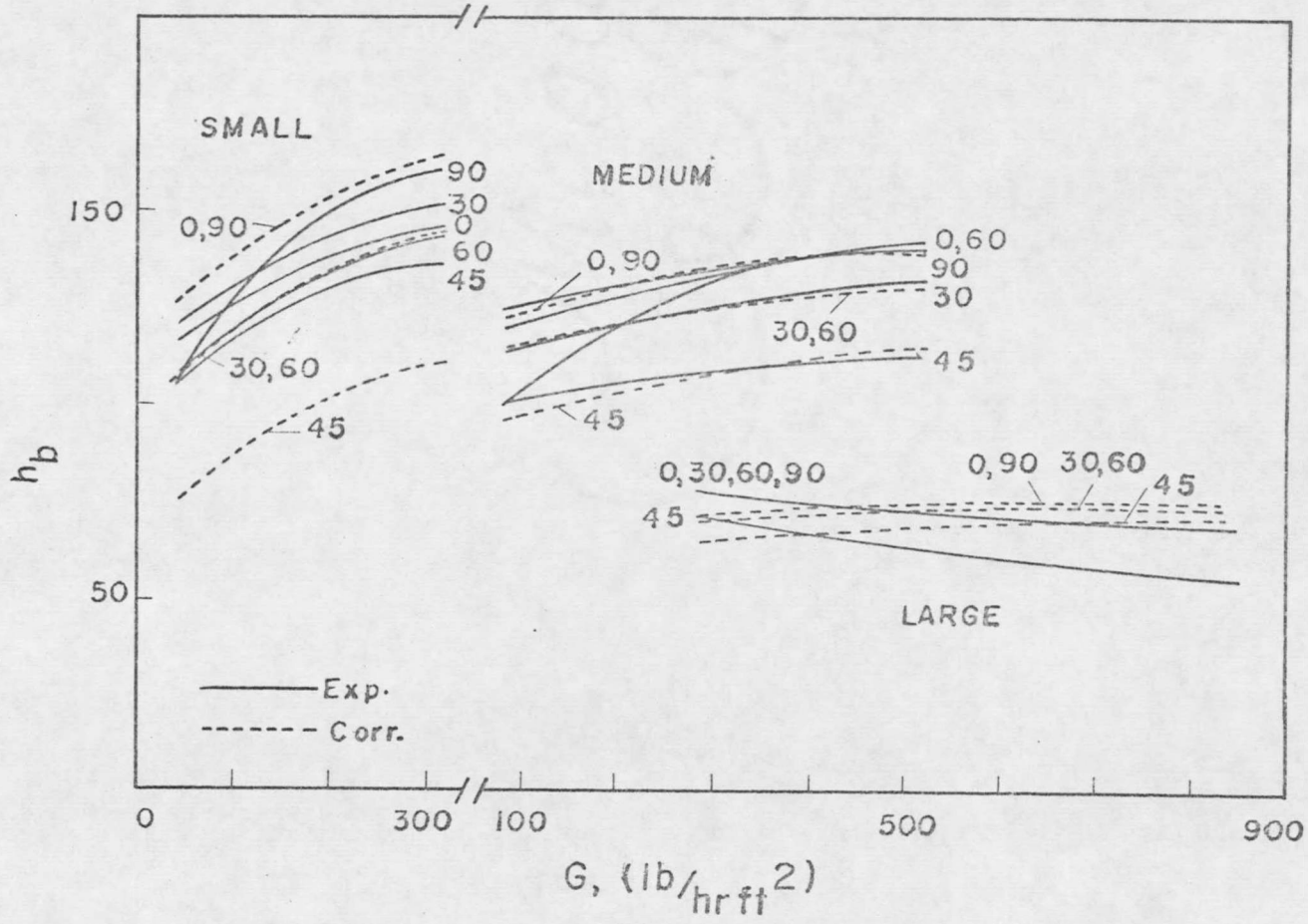


FIGURE 20. COMPARISON OF EXPERIMENTAL h_b's AND PREDICTED VALUES FROM THE AUTHOR'S CORRELATION (BARE TUBE).

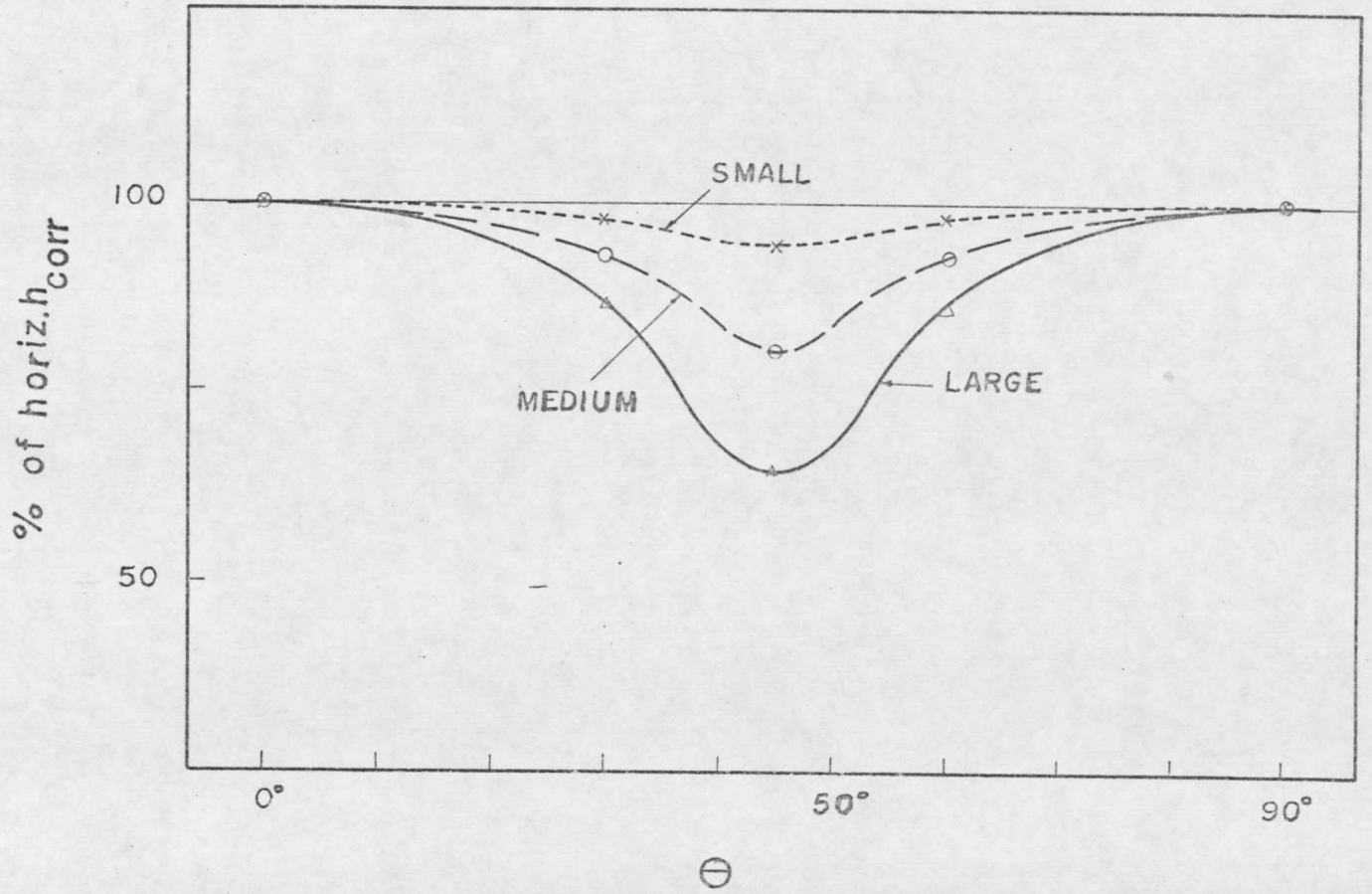


FIGURE 21. PREDICTED EFFECT OF ANGLE ON HEAT TRANSFER COEFFICIENTS OF BARE TUBE.

wall of the tube, the fin effectiveness factor, ϕ, would approach unity. Unity would not necessarily be reached, however, because fins affect the coefficients by affecting the fluidization around the tube. In this hypothetical situation, the conventional fin efficiency would be unity because the ΔT at the fin tips would be the same as the ΔT at the base of the fins. The effectiveness factor is a better parameter than fin efficiency for fluidized bed studies because it does account for the effect of fins on fluidization.

If it is remembered that the ΔT in the equation is between the bed and the wall of the tube, a pseudo-coefficient, h_{ff}, can be used for discussion purposes. This is the coefficient of the finned tube based on the total area of the tube. In this case the term $(h_b \phi)$ would equal h_{ff}; both being equal to $q/A_f(\Delta T)$. So it can be seen that ϕ is determined experimentally and is equal to h_{ff}/h_b.

The results of examining the finned tube at the same five angles and same conditions as the bare tube are shown in Figures 22 and 23. In these Figures the heat transfer coefficients of the finned tube based on the total area, h_{ff}'s, and the actual coefficients, h_f's, which were found by using the analytical procedure presented earlier are plotted versus mass flow rate. Values for the different angles and particle sizes are shown. To obtain values of ϕ, the

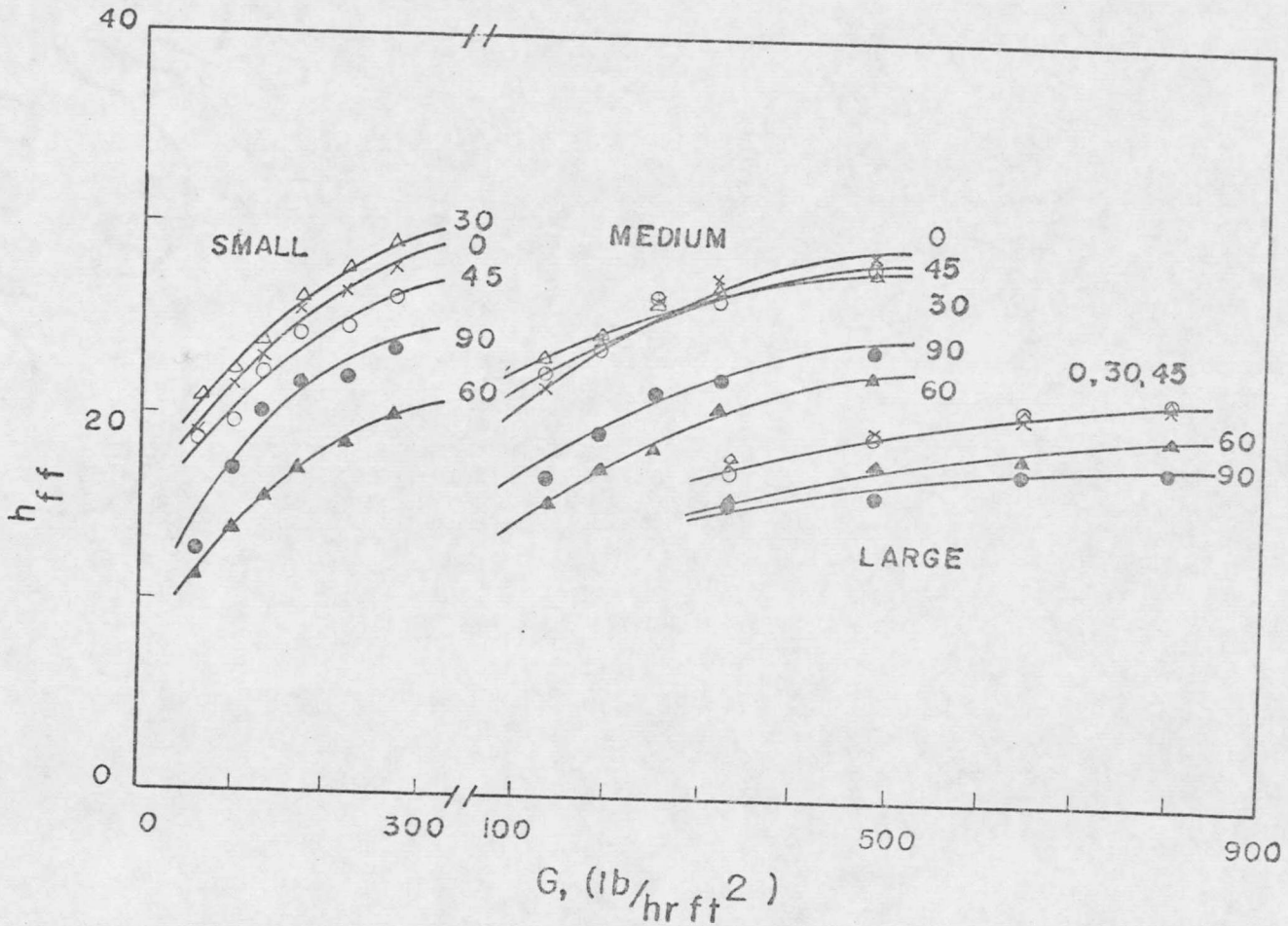


FIGURE 22. RESULTS OF h_{ff} FROM FINNED TUBE STUDY.

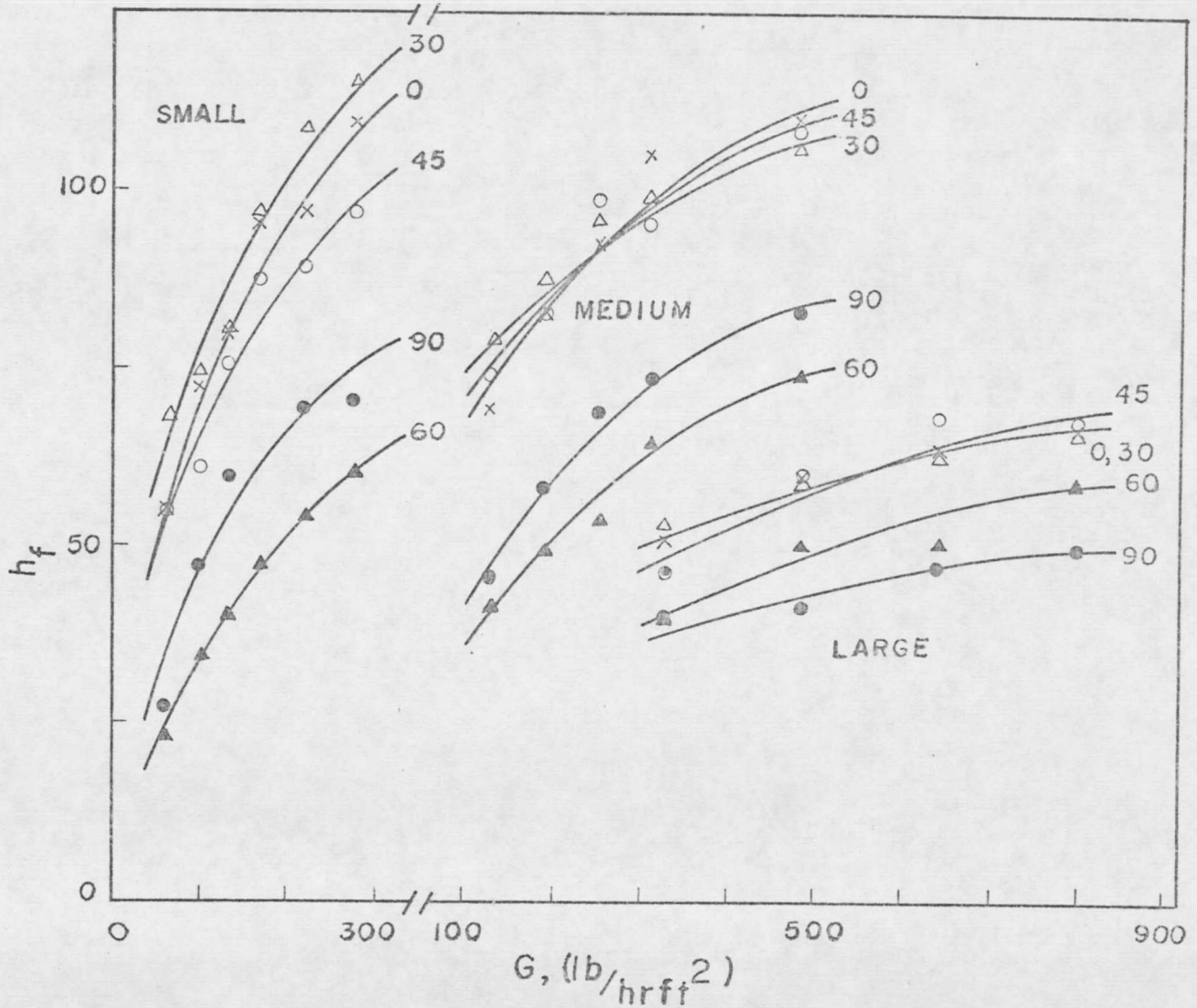


FIGURE 23. RESULTS OF h_f FROM FINNED TUBE STUDY.

effectiveness factor, values of h_{ff} were taken from Figure 22 and divided by the corresponding value of h_b from Figure 16. Figure 24 shows the effectiveness factor plotted versus mass flow rate for different particle sizes and angles; its value ranges between 0.1 and 0.4.

From Figures 22 and 23 it is evident that while the coefficients are nearly the same for the first three angles (0°, 30°, and 45°), the 60° and 90° positions give substantially lower coefficients. Coefficients for the vertical tube are on the average 18.9% lower than the horizontal coefficients for the small particles; 18.2% lower than horizontal for the medium particles; and 15.6% lower for the large particles. The 60° tube position using the small particles gave heat transfer coefficients approximately 32% lower than tubes in the horizontal position and for the medium size particles it was about 24% lower.

It is interesting to note that for the two smaller particle sizes the 60° tube position gives the lowest coefficients whereas the 90° tube position gives the lowest coefficients when using the largest particles. This might possibly be explained by particle hold-up.

In the case of the two smaller particle sizes, a minimum coefficient is reached at a 60° tube angle, possibly due to regions of

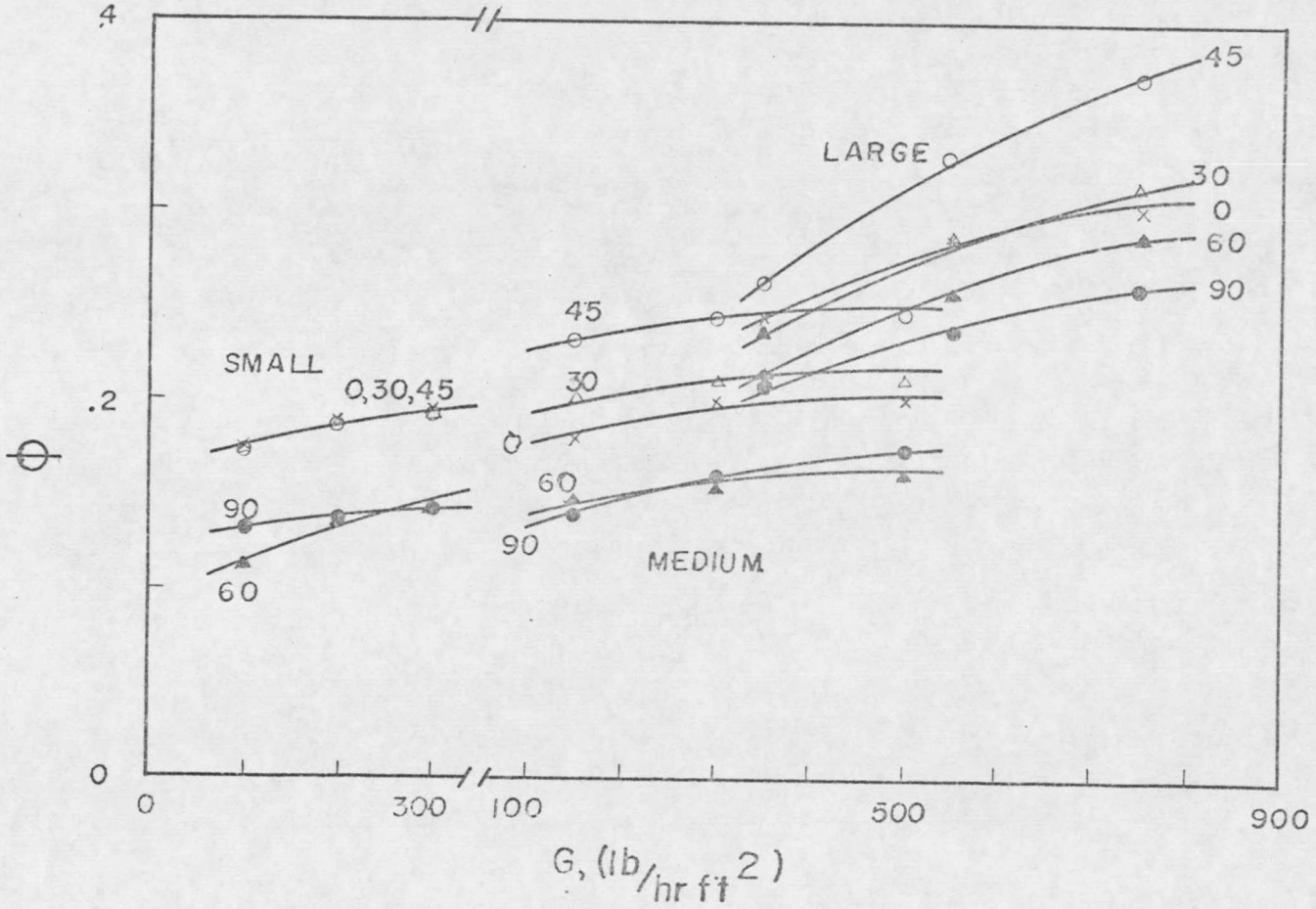


FIGURE 24. RESULTING EFFECTIVENESS FACTORS FROM BARE AND FINNED TUBE STUDIES.

poor fluidization resulting from the geometry of the tube. In the vertical tube position fluidization increases around the tube and transfer increases. In the case of the large particles, the same situation would probably exist if not for particle hold-up on the fins. (Fins are horizontal when tube is in vertical position.) Since the large particles are 2 to 4 times the size of the smaller ones, they may not be moved rapidly off the fin by the fluid motion. This would cause increased particle contact time and "dead" spots on the fins. Another factor is that the large particles may have difficulty moving between the fins -- the only paths available in the vertical position. This could cause a decrease in heat transfer because of less particle movement.

Experimental results of the finned tube examination are compared in Figures 25 and 26 with those predicted by the author's correlation. The average deviation of the experimental values from the predicted values in Figure 25 is 6.2 per cent.

The effect of tube angle on the heat transfer coefficient of finned tubes as predicted by the correlation is shown in Figure 27. In the Figure, the value of the coefficient is expressed as a per cent of the horizontal coefficient and is plotted versus angle for each particle size.

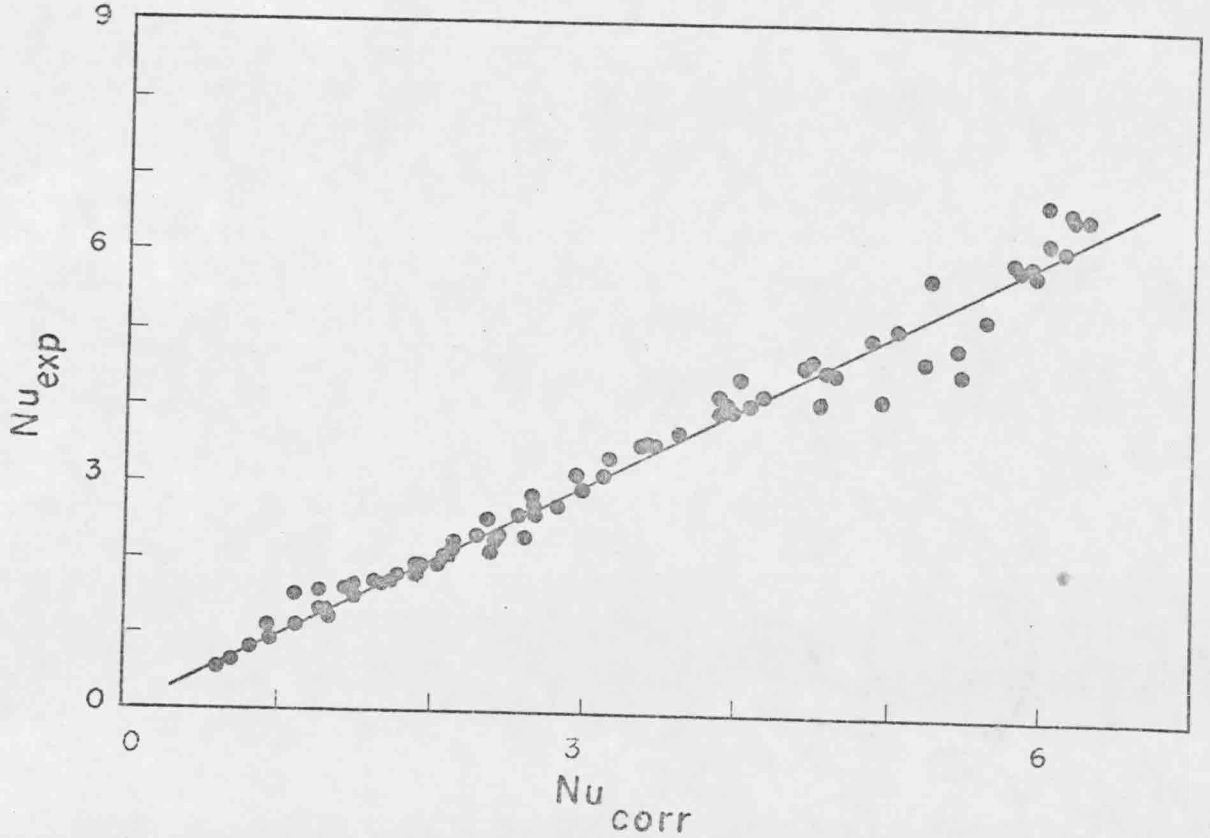


FIGURE 25. COMPARISON OF EXPERIMENTAL Nu's AND THE AUTHOR'S CORRELATION (FINNED TUBE).

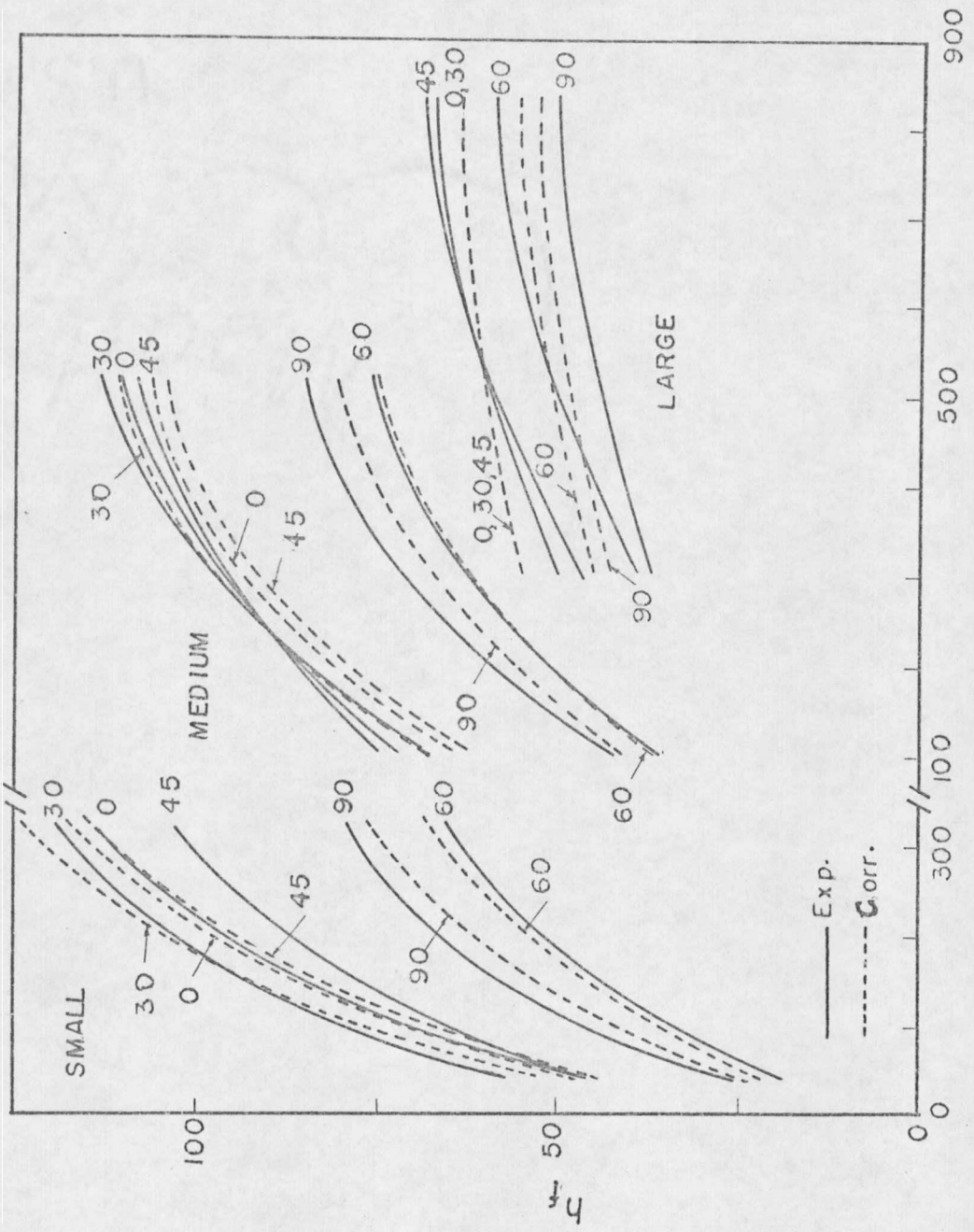


FIGURE 26. COMPARISON OF EXPERIMENTAL h_f's AND PREDICTED VALUES FROM THE AUTHOR'S CORRELATION (FINNED TUBE).

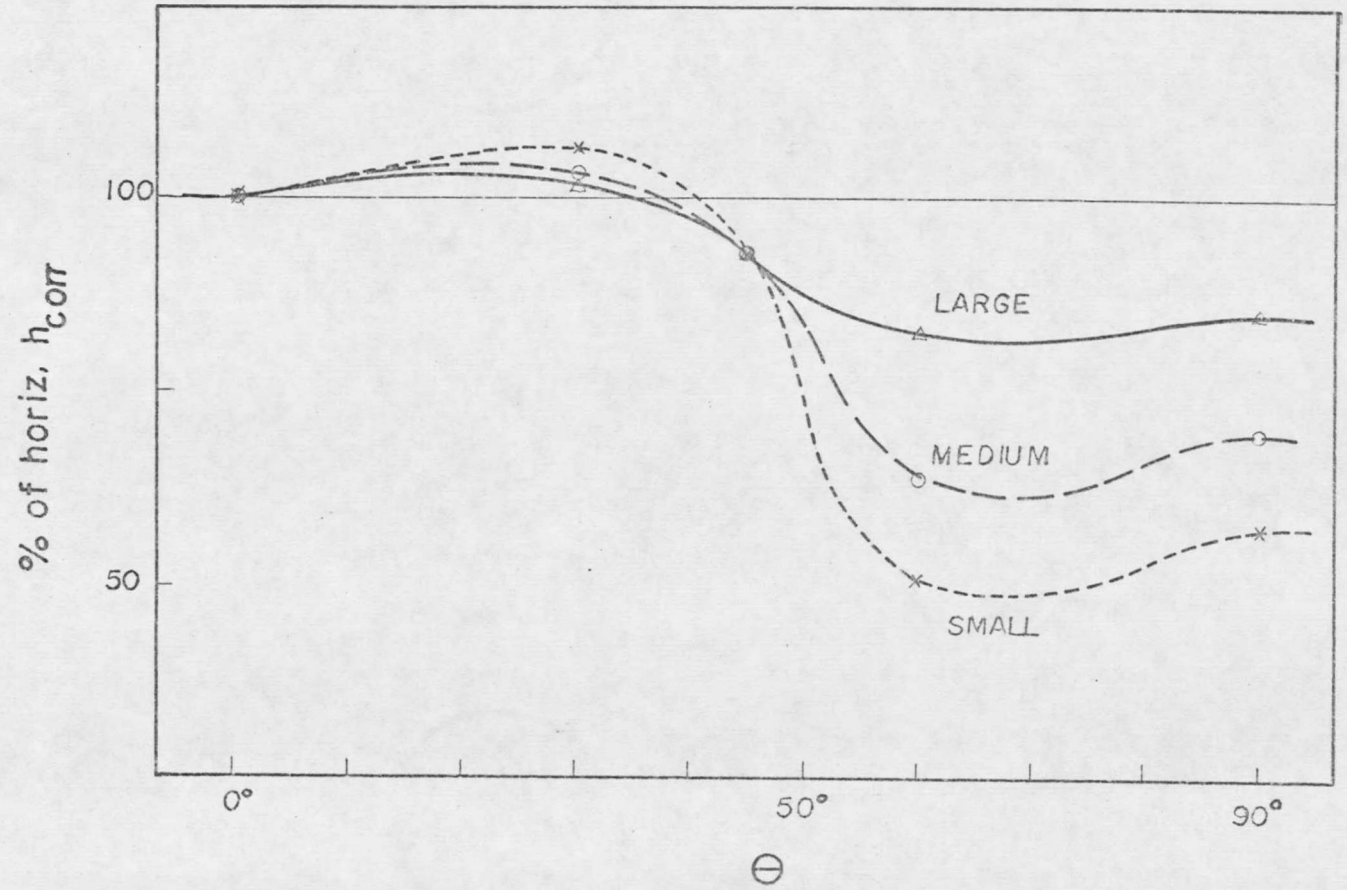


FIGURE 27. PREDICTED EFFECT OF ANGLE ON HEAT TRANSFER COEFFICIENTS OF FINNED TUBE.

A brief examination was made on a copper-clad finned tube described in the section on equipment. The main purpose was to determine how much the increased thermal conductivity of the extended surface would affect the heat transfer rate. Since the copper-clad tube had different dimensions and fin spacing, an accurate comparison could not be made; however, by comparing the heat transfer coefficients based on the total area (h_{ff}'s), the effect of fin conductivity can be approximated. A comparison of the two finned tubes both in the horizontal position is shown in Figure 28. It can be seen that the coefficient is from 1-1/2 to nearly 2 times as great.

Ziegler et al (22) predicted a maximum Nusselt number of 7.2; this value was slightly exceeded in this experiment. The highest Nusselt number obtained here was 7.79.

Sources of Error

Probably the most serious source of error was the fact that the internal heaters did not contact the inside tube wall uniformly. This may have resulted in cool spots on the tube which would give erroneous temperature measurements.

Inaccurate measurement of air flow into the column was another possible source of error because the rotometers were difficult to read accurately. The vertical pressure drop measurement with the

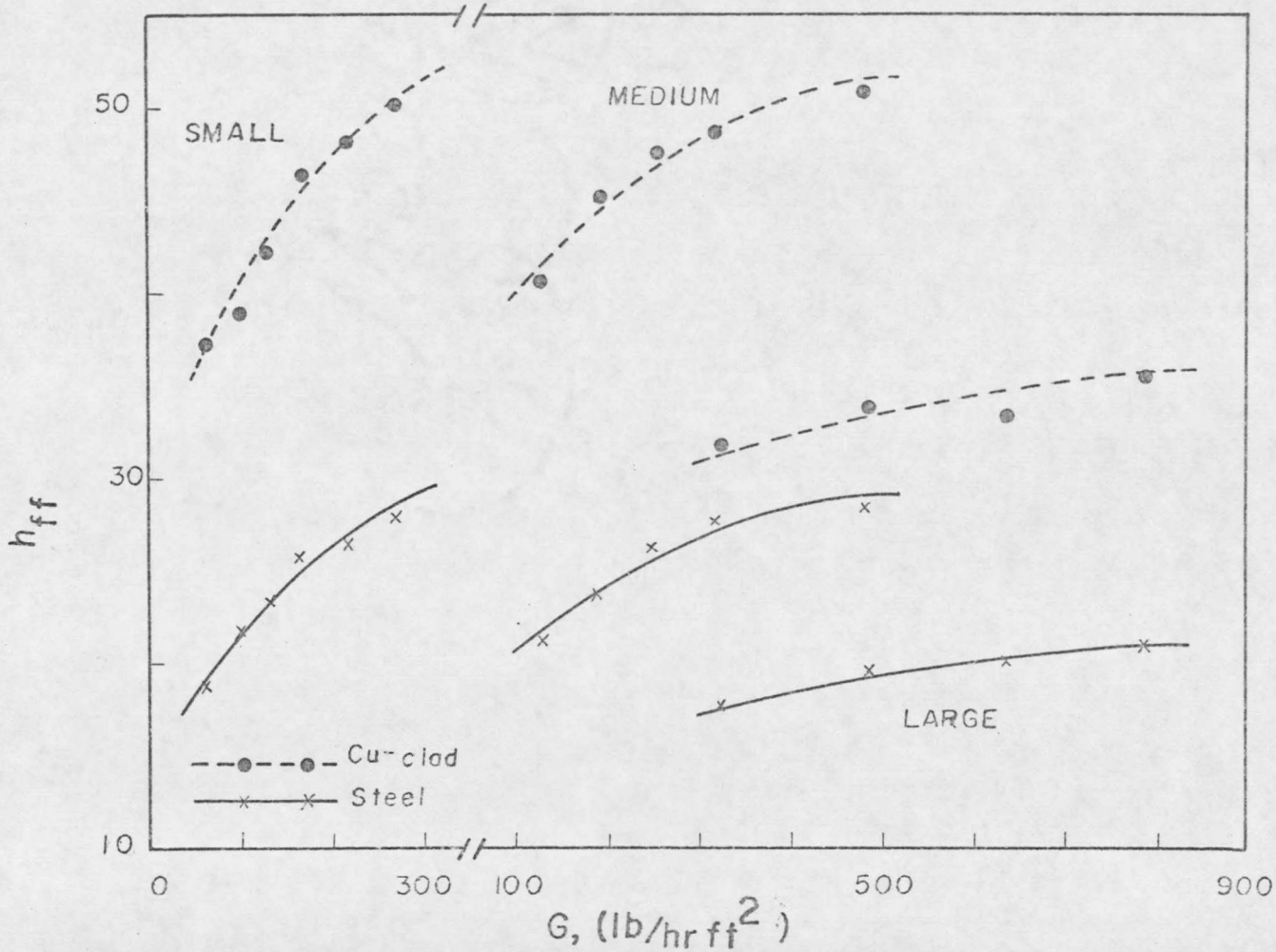


FIGURE 28. EFFECT OF INCREASED THERMAL CONDUCTIVITY ON HEAT TRANSFER.

manometers was affected by movement of the water levels, and by the particle hold-up due to the baffle plate. Static charges affected this reading also by holding particles to the plastic column wall.

The motion of particles may have been slightly influenced by the presence of the insulation on the ends of the tubes. Other measurements are believed to be accurate.

Conclusions

1. Generally, the heat transfer coefficient increases with mass flow rate. Other investigators have shown this to be true with a maximum value being reached, followed by a declining value.

2. At a given air flow rate (which is less than that for the maximum h), heat transfer varies inversely with particle size.

3. A 45° position resulted in minimum heat transfer for the bare tube studied. A 60° position produced minimum results for the finned tube with the two smaller particle sizes.

4. A correlation for determining heat transfer coefficients from bare tubes at various orientations in a fluidized bed is:

$$Nu = \frac{11\ (1-\epsilon)^{1/2}}{\left[1 + \frac{.44 - .20\ (\theta-45)^2}{(\theta-45)^2 + 120}\right]^2 Re^{.24}\left(\frac{D_p}{.008}\right)^{1.23}}$$

where D_p is expressed in inches.

5. A correlation for determining heat transfer coefficients from the finned tube under study in a fluidized bed is:

$$Nu = \frac{11\,(1-\epsilon)^{1/2}}{\left[\,1 + \dfrac{C}{Re^{.51}\left(\dfrac{D_p}{.008}\right)^{.35}}\,\right]^2}$$

where C is a function of angle and D_p is expressed in inches.

6. Increased thermal conductivity of the fins increases the heat transfer rate of finned tubes substantially.

7. By knowing the effect of orientation on the heat transfer coefficients of single bare and finned tubes, a more sound decision on bundle design can be made.

Investigations of tube bundle design in a fluidized bed would be valuable for design and are recommended by the author for further study.

BIBLIOGRAPHY

BIBLIOGRAPHY

1. Baddour, R. F., and C. Y. Yoon, "Local Radial Effective Conductivity and the Wall Effect in Packed Beds," A.I.Ch.E., Chemical Engineering Progress, Symposium Series No. 32, p. 35-50, 1961. (Supplement to Chemical Engineering Progress v. 57).

2. Botterill, J. S., and J. R. Williams, "The Mechanism of Heat Transfer to Gas-Fluidized Beds," Transactions of the Institution of Chemical Engineers, 41: 217-230, June, 1963.

3. Dow, Willard, and Max Jakob, "Heat Transfer Between a Vertical Tube and a Fluidized Air-Solid Mixture," Chemical Engineering Progress, 47: 637-648, December, 1951.

4. Gampson, Bernard W., "Heat and Mass Transfer," Chemical Engineering Progress, 47: 19-28, 1951.

5. Genetti, William E., "Heat Transfer in a Fluidized Bed Heat Exchanger." Dissertation, Oregon State University, Corvallis, Oregon, 1968, 177 pp.

6. Kunii and Levenspiel, Fluidization Engineering. New York: John Wiley and Sons, Inc., 1969, 534 pp.

7. Leva, Max, Fluidization. New York: McGraw-Hill Book Co., Inc., 1959, 327 pp.

8. Leva, Max, M. Weintraub, and M. Grummer, "Heat Transmission Through Fluidized Beds of Fine Particles," Chemical Engineering Progress, 45: 563-572, September, 1949.

9. Levenspiel, O., and J. S. Walton, "Bed-Wall Heat Transfer in Fluidized Systems," A.I.Ch.E., Chemical Engineering Progress, Symposium Series No. 9, p. 1-13, 1954. (Supplement to Chemical Engineering Progress v. 50).

10. Mickley, H. S., and D. F. Fairbanks, "Mechanism of Heat Transfer to Fluidized Beds," A.I.Ch.E. Journal, 1: 374-384, September, 1955.

11. Mickley, H. S., and Charles A. Trilling, "Heat Transfer Characteristics of Fluidized Beds," Industrial and Engineering Chemistry, 41: 1135-1147, June, 1949.

BIBLIOGRAPHY (continued)

12. McAdams, William H., Heat Transmission. New York: McGraw-Hill Book Co., Inc., 1954, 532 pp.

13. Nöe, A. R., "Local and Average Heat Transfer Coefficients in a Fluidized Bed Heat Exchanger." Unpublished Masters Thesis, Oregon State University, Corvallis, Oregon, 1964, 88 pp.

14. Petrie, Freeby, and Buckham, "In Bed Heat Exchangers," Chemical Engineering Progress, 64: 45-51, July, 1966.

15. Sharai, Yoshitome, Shoji, Tanaka, Hojo, and Yoshida, "Heat and Mass Transfer on the Surface of Solid Spheres Fixed Within Fluidized Beds," Kagaku Kōgaku, (Chemical Engineering -- Japan, abridged English edition), 4: 162-165, Spring, 1966.

16. Toomey, R. D., and H. F. Johnstone, "Heat Transfer Between Beds of Fluidized Solids and the Walls of the Container," A.I.Ch.E., Chemical Engineering Progress, Symposium Series No. 5, p. 51-63, 1953. (Supplement to Chemical Engineering Progress v. 49).

17. Van Heerden, C., A. P. Nobel, and D. W. van Krevelen, "Mechanism of Heat Transfer in Fluidized Beds," Industrial and Engineering Chemistry, 45: 1237-1242, June, 1953.

18. Vreedenberg, H. A., "Heat Transfer Between a Fluidized Bed and a Horizontal Tube," Chemical Engineering Science, 9: 52-60, August, 1958.

19. Wender, Leonard, and George T. Cooper, "Heat Transfer Between Fluidized Beds on Boundary Surfaces -- Correlation of Data," A.I.Ch.E. Journal, 4: 15-23, March, 1958.

20. Zenz, and Othmer, Fluidization and Fluid Particle Systems. New York: Reinhold Co., 1960, 444 pp.

21. Ziegler, E. N., and W. T. Brazelton, "Mechanism of Heat Transfer to a Fixed Surface in a Fluidized Bed," Industrial and Engineering Chemistry Fundamentals, 3: 94-98, May, 1964.

22. Ziegler, E. N., L. B. Koppel, and W. T. Brazelton, "Effects of Thermal Properties on Heat Transfer to Gas Fluidized Beds," Industrial and Engineering Chemistry Fundamentals, 3: 324-328, November, 1964.

APPENDIX

NOMENCLATURE

Symbol	Definition	Dimensions
a	exponent on particle Reynolds number	dimensionless
A	area of transfer surface	ft^2
A_{bf}	area of the base of one fin	ft^2
A_f	total area of finned tube	ft^2
A_w	area of tube wall	ft^2
Amps	current in heater circuit	Amperes
b	exponent on $(D_p/.008)$, where D_p is in inches	dimensionless
B	Subscript indicating big rotometer	"
c_1, c_2	constants in general solution to differential equation	dimensionless
C	function of tube angle, equal to $F\ Re^{-a}\ (D_p/.008)^{-b}$	dimensionless
C_{pg}	heat capacity of fluid	BTU/lb-^oF
C_{ps}	heat capacity of solid particles	BTU/lb-^oF
cosh	hyperbolic cosine function	dimensionless
C_R	constant, assumed to be unity	dimensionless
D_f	diameter of fluidizing column	ft, inches
D_p	particle diameter	ft, inches
D_t	tube diameter	ft, inches
F	dimensionless group equal to $C\ Re^{a}\ (D_p/.008)^{b}$	dimensionless

NOMENCLATURE (continued)

Symbol	Definition	Dimensions
g	gravitational acceleration, 4.18×10^8	ft/hr^2
G	mass flow rate	$lb/hr\text{-}ft^2$
G_{mf}	mass flow rate at minimum fluidization	$lb/hr\text{-}ft^2$
h	heat transfer coefficient	$BTU/hr\text{-}ft^2\text{-}F^\circ$
h_b	heat transfer coefficient of base tube	$BTU/hr\text{-}ft^2\text{-}F^\circ$
h_{ff}	heat transfer coefficient based on total area of finned tube and (T_w-T_b)	$BTU/hr\text{-}ft^2\text{-}F^\circ$
h_f	heat transfer coefficient of finned tube	$BTU/hr\text{-}ft^2\text{-}F^\circ$
h_{corr}	heat transfer coefficient from author's correlation	$BTU/hr\text{-}ft^2\text{-}F^\circ$
Δh, Δh_2	water level height differences	ft, inches
k	thermal conductivity	$BTU/hr\text{-}ft\text{-}F^\circ$
k_g	thermal conductivity of fluid	$BTU/hr\text{-}ft\text{-}F^\circ$
k_s	thermal conductivity of solid particles	$BTU/hr\text{-}ft\text{-}F^\circ$
l	length of fin	ft, inches
L	distance between pressure taps	ft, inches
L_h	length of transfer surface	ft, inches
L_f	height of bubbling bed	ft, inches
m	group equal to $\frac{2h\ (\delta+\omega)}{k\omega\delta}$	ft^{-2}

NOMENCLATURE (continued)

Symbol	Definition	Dimensions
N	total number of fins on tube	dimensionless
Nu_{corr}	particle Nusselt number calculated from author's correlation	dimensionless
Nu_{exp}	particle Nusselt number calculated from experimental data	dimensionless
Nu_p	particle Nusselt number, $h D_p/k$	dimensionless
P_1, P_2	pressure upstream and downstream from rotometer and valves	lb/in^2
Pr	Prandtl number, $C_{pg}\mu/k$	dimensionless
Δp	pressure drop between pressure taps	lb/in^2
q	rate of heat transfer	BTU/hr
q_f	rate of heat transfer from one fin	BTU/hr
q_t	rate of heat transfer from entire finned tube	BTU/hr
q_w	rate of heat transfer from tube wall	BTU/hr
Re	particle Reynolds number, $D_p G/\mu$	dimensionless
Roto	reading on rotometer scale	dimensionless
s	subscript indicating small rotometer	dimensionless
SCFM	standard cubic feet per minute	ft^3/min
sinh	hyperbolic sin function	dimensionless
T	temperature at any point on the fin	^oF
T_b	temperature of the bed	^oF
$T_1 \ldots T_5$	temperatures at thermocouple locations	^oF

NOMENCLATURE (continued)

Symbol	Definition	Dimensions
T_{av}	average temperature of tube	^{o}F
ΔT_{av}	mean tube temperature minus the bed temperature	^{o}F
T_{w}	temperature at the wall of the tube	^{o}F
$\bar{t}$	mean residence time	sec
U_{o}	superficial fluid velocity	cm/sec
U_{mf}	superficial fluid velocity at minimum fluidization	cm/sec
Volts	potential across heater circuit	volts
x	distance from tube wall	ft, inches
Δx	thickness of differential element	ft, inches
δ	width of differential element	ft, inches
ϵ	void fraction	dimensionless
ϵ_{mf}	void fraction at minimum fluidization	dimensionless
$(1-\epsilon)$	particle fraction	dimensionless
θ	angle of tube with respect to the horizontal	degrees
ρ_{g}	density of fluid	lb/ft^3
ρ_{s}	density of solid	lb/ft^3
μ	viscosity	lb/ft-hr
ϕ	fin effectiveness factor	dimensionless
ω	length of differential element	ft, inches

COMMENTS

A preliminary examination showed that there was a slight temperature gradient around the tube. This was the basis for the thermocouple locations used.

Most of the runs were made with another heating tube present in the bed. A preliminary study showed that there was no effect on the author's tube due to the presence of the second tube.

Per cent deviations given are all based on the premise that the correlations are correct.

EQUIPMENT

Pressure Gauge (upstream from rotometers):

Bronze tube Duragauge -- Ashcroft

2 lb. subd., Full scale: 160 lbs.

Pressure Gauge (downstream from rotometers):

Acco Helcoid Gauge

4-1/2 W-60-0.5 lb subd., Full scale: 60 lbs.

Small Rotometer:

Brooks -- 9 RM 25 5

Full scale: 13.45 SCFM

Large Rotometer:

Brooks -- 1110, Serial No. 31176

13 RM 25.1, Full scale: 108.3 SCFM

Manometers:

Meriam Instrument Co.

Fluid: Water

Voltmeter:

Daystrom, Inc., Weston Instruments

Full scale: 150 volts

Ammeter:

Daystrom, Inc., Weston Instruments

Range: 0-5 amps.

Powerstat:

Superior Electric Company

120 volt, Type 116

EQUIPMENT (continued)

Thermocouples:

Iron-Constantan

Temperature Recorder:

Brystol Dynamaster, 66A-68A-473

Model: 2PGPG550-21-21-TH85A-NH3A

Calrod Heater:

Firerod Heater, Watlow Co.

240 v. 1000 watt, J9AX

Finned Tubes:

Escoa Corporation

Pryor, Oklahoma

Glass Beads:

3-M Company; .0045", .0080", and .0185" in diam.

SAMPLE DATA SHEET

EXPERIMENT LOG Date 8/25/69

Run No's. 40-45 Written up by Rod Schmall

Tube Type Finned Particle Size Small

Tube Angle 45° Tube Height 16 in.

Run No.	40	41	42	43	44	45
P_1	19.5	19.5	19.5	19.0	18.5	18.5
P_2	1.6	1.7	1.9	2.0	2.3	2.8
Roto	48_S	72_S	96_S	15_B	20_B	25_B
Δh_1	9.8	9.8	9.6	9.4	9.4	9.0
Δh_2	14.6	14.6	14.6	14.6	14.6	14.3
Amps	1.92	2.11	2.27	2.37	2.45	2.47
Volts	104.1	114.8	123.0	128.8	133.0	134.0
T_b	145.0	144.5	143.0	138.0	134.5	129.0
T_1	171.5	174.5	174.5	171.0	170.0	163.0
T_2	*178.0	181.0	179.0	172.5	171.0	164.0
T_3	180.5	181.5	182.0	176.5	175.0	168.0
T_4	170.0	174.5	171.5	165.0	163.0	156.5
T_5	167.5	171.0	169.0	163.5	161.5	155.0

*This temperature varied from 175-181 $^{\circ}$F.

TEMPERATURE

Development of Average for Finned Tube

If temperatures at the end are assumed to vary around the tube at the ends the same as in the middle, the twelve temperatures can be expressed as

1	T_1	top temperatures
2	T_2	
3	T_3	
4	$T_1 - (T_2-T_4)$	front side temperatures
5	T_4	
6	$T_3 - (T_2-T_4)$	
7	$T_1 - (T_2-T_4)$	back side temperatures
8	T_4	
9	$T_3 - (T_2-T_4)$	
10	$T_1 - (T_2-T_5)$	bottom temperatures
11	T_5	
12	$T_3 - (T_2-T_5)$	

Adding all twelve gives:

$$T_1 + T_2 + T_3 + T_1 - T_2 + T_4 + T_4 + T_3 - T_2 + T_4 + T_1 - T_2$$

$$+ T_4 + T_4 + T_3 - T_2 + T_4 + T_1 - T_2 + T_5 + T_5 + T_3 - T_2 + T_5$$

Collecting terms gives:

$$4T_1 + 4T_3 + 6\,T_4 + 3T_5 - 5T_2$$

Thus the average of these twelve points is

$$T_{av} = 1/12\ (4T_1 + 4T_3 + 6T_4 + 3T_5 - 5T_2)$$

PARTICLE FRACTION

All the runs made at a given flow rate were used to determine the average particle fraction at that rate.

Particle Size	G	$(1-\epsilon)_{av}$
Small	65	.517
	98	.511
	129	.506
	163	.505
	217	.501
	270	.496
Medium	128	.522
	191	.517
	250	.515
	312	.510
	481	.506
Large	326	.503
	485	.503
	641	.501
	795	.502

Q/Δ T VALUES FROM ARBITRARY COEFFICIENTS
USING ANALYTICAL PROCEDURE

h	Q/Δ T
5	5.42
10	9.22
15	12.2
20	14.7
25	16.9
30	18.9
35	20.7
40	22.4
45	24.0
50	25.5
55	27.0
60	28.4
65	29.8
70	31.1
75	32.4
80	33.7
85	34.9
90	36.1
95	37.3
100	38.4
105	39.6
110	40.7
115	41.8
120	42.9
125	44.0
130	45.0
135	46.1
140	47.1
145	48.1
150	49.1

COEFFICIENTS FROM CORRELATIONS FOR HORIZONTAL BARE TUBE

Particle Size	G	Experimental h_b	Zenz-Othmer h_b	Zenz-Othmer % Dev	Vreedenberg h_b	Vreedenberg % Dev
Small	70	122	154	20.8	102	19.6
	100	126	172	26.7	113	11.5
	150	133	197	32.5	128	3.9
	200	139	217	35.9	139	0.0
	250	143	234	38.9	149	4.0
	300	148	248	40.3	158	6.3
		average:		32.6		7.6
Medium	100	122	93.4	30.6	67.5	80.7
	150	126	107	17.8	76.2	65.4
	200	130	117	11.1	83.1	56.4
	250	133	126	5.6	88.8	49.8
	300	135	134	0.7	93.8	43.9
	400	139	148	6.1	102.0	36.3
	500	140	159	11.9	109.0	28.4
		average:		12.0		51.6
Large	300	74	39.7	86.4	44.1	67.8
	500	72	57.4	25.4	51.4	40.1
	600	72	61.0	18.0	54.3	32.6
	800	71	67.0	6.0	59.2	19.9
		average:		34.0		40.1

COEFFICIENTS FROM CORRELATION FOR VERTICAL BARE TUBE

Particle Size	G	Experimental h_b	Vreedenberg h_b	% Deviation
Small	70	112	98.7	13.5
	100	126	107	17.8
	150	143	118	21.2
	200	153	126	21.4
	250	159	132	20.5
	300	162	138	17.4
			average:	18.6
Medium	100	120	69.8	71.9
	150	127	76.7	65.6
	200	131	81.9	60.0
	250	135	86.3	56.4
	300	137	90.0	52.2
	400	138	96.1	43.6
	500	138	101	36.6
			average:	55.2
Large	300	82	46	78.3
	500	74	51.8	42.9
	600	71	54	31.5
	800	69	57.7	19.6
			average:	43.1

EFFECTIVENESS FACTORS

Particle Size	Tube Angle	G	ϕ ($\phi = h_{ff}/h_b$)
Small	0°	100	.173
		200	.190
		300	.195
	30°	100	.174
		200	.189
		300	.193
	45°	100	.178
		200	.185
		300	.191
	60°	100	.114
		200	.134
		300	.143
	90°	100	.132
		200	.138
		200	.143
Medium	0°	150	.181
		300	.201
		500	.201
	30°	150	.201
		300	.210
		500	.211
	45°	150	.233
		300	.245
		500	.246
	60°	150	.148
		300	.154
		500	.161
	90°	150	.140
		300	.161
		500	.174

EFFECTIVENESS FACTORS (continued)

Particle Size	Tube Angle	G	ϕ ($\phi = h_{ff}/h_b$)
Large	0°	350	.245
		550	.286
		750	.301
	30°	350	.238
		550	.286
		750	.315
	45°	350	.262
		550	.327
		750	.370
	60°	350	.214
		550	.258
		750	.288
	90°	350	.208
		550	.237
		750	.260

PREDICTED EFFECT OF ANGLE

Tube Type	Particle Size	Tube Angle	% of Horizontal h_{corr}
Bare	Large	0	100
		30	86
		45	64
		60	86
		90	100
	Medium	30	93
		45	80
		60	93
		90	100
	Small	30	98
		45	94
		60	98
		90	100
Finned	Large	0	100
		30	102
		45	99
		60	83
		90	86
	Medium	30	104
		45	99
		60	64
		90	70
	Small	30	107
		45	98
		60	51
		90	58

RECORDED AND CALCULATED DATA

Tube Type: Finned
Tube Angle: 0^{o}

Run No.	Particle Size	G	$q/\Delta T_{av}$	h_{ff}	h_f	h_{corr}	Re	F	F/Re^a	Nu_{exp}	Nu_{corr}	% Dev.
1	Large	326	25.8	17.9	50.8	56.1	10.9	.250	.847	4.99	5.51	9.38
2	Large	485	28.4	19.6	60.0	59.5	16.3	.150	.623	5.89	5.84	0.85
3	Large	641	29.3	20.3	63.3	61.6	21.5	.119	.569	6.22	6.05	2.79
4	Large	795	30.3	21.0	66.8	63.2	26.7	.090	.480	6.56	6.21	5.71
5	Medium	129	31.0	21.5	69.5	70.4	1.86	.641	.878	2.95	2.99	1.33
6	Medium	190	34.4	23.9	83.0	81.3	2.77	.498	.837	3.53	3.45	2.12
7	Medium	250	37.9	26.3	92.6	88.7	3.63	.416	.803	3.93	3.77	4.44
8	Medium	312	39.6	27.5	105.0	94.4	4.52	.327	.706	4.46	4.01	11.2
9	Medium	481	40.5	28.1	110.0	105.6	6.97	.294	.791	4.67	4.48	4.18
10	Small	64.7	27.3	18.9	56.0	54.8	0.53	1.43	1.04	1.34	1.31	2.28
11	Small	97.1	31.7	21.9	72.2	69.0	0.80	1.14	1.01	1.72	1.65	4.58
12	Small	130	33.8	23.4	80.5	79.6	1.05	1.02	1.04	1.92	1.90	1.11
13	Small	164	37.3	25.9	95.1	89.4	1.33	.855	.989	2.27	2.14	6.32
14	Small	217	37.7	26.2	97.0	101.8	1.77	.833	1.11	2.32	2.43	4.74
15	Small	271	40.3	27.9	109.3	111.4	2.20	.722	1.08	2.61	2.66	1.91
16	Large	323	26.5	18.4	53.2	57.3	10.9	.222	.750	5.23	5.63	7.20
17	Large	480	28.2	19.5	59.3	60.6	16.3	.157	.651	5.82	5.95	2.18
18	Large	641	29.1	20.1	62.5	62.6	21.5	.126	.603	6.14	6.15	0.18
19	Large	788	30.3	21.0	66.8	64.2	26.7	.090	.480	6.56	6.30	4.12

Tube Type: Finned
Tube Angle: 30°

Run No.	Particle Size	G	$q/\Delta T_{av}$	h_{ff}	h_f	h_{corr}	Re	F	F/Re^a	Nu_{exp}	Nu_{corr}	% Dev.
16	Large	323	26.5	18.4	53.2	57.3	10.9	.222	.750	5.23	5.63	7.20
17	Large	480	28.2	19.5	59.3	60.6	16.3	.157	.651	5.82	5.95	2.18
18	Large	641	29.1	20.1	62.5	62.6	21.5	.126	.603	6.14	6.15	0.18
19	Large	788	30.3	21.0	66.8	64.2	26.7	.090	.480	6.56	6.30	4.12
20	Medium	127	33.4	23.1	79.1	74.4	1.86	.538	.737	3.36	3.16	6.32
21	Medium	190	35.4	24.5	87.2	85.3	2.77	.461	.775	3.70	3.62	2.27
22	Medium	250	37.5	26.0	96.1	92.6	3.63	.390	.753	4.08	3.93	3.77
23	Medium	312	38.2	26.5	99.0	98.3	4.52	.367	.792	4.21	4.17	0.74
24	Medium	481	39.8	27.5	106.0	109.3	6.97	.318	.856	4.50	4.64	2.98
25	Small	65.2	30.6	21.2	68.0	59.6	0.53	1.21	.873	1.62	1.42	14.1
26	Small	97.8	32.4	22.5	75.0	74.6	0.80	1.10	.977	1.79	1.78	0.57
27	Small	129	34.1	23.6	81.8	85.6	1.05	1.00	1.03	1.95	2.04	4.40
28	Small	163	37.8	26.2	97.3	95.7	1.33	.834	.964	2.32	2.29	1.66
29	Small	215	40.2	27.9	108.7	108.4	1.77	.732	.979	2.60	2.59	0.29
30	Small	269	41.8	29.0	115.0	118.2	2.20	.679	1.02	2.75	2.82	2.67

Tube Type: Finned

Tube Angle: 45°

Run No.	Particle Size	G	$q/\Delta T_{av}$	h_{ff}	h_f	h_{corr}	Re	F	F/Re^a	Nu_{exp}	Nu_{corr}	% Dev.
31	Large	323	24.3	16.8	45.9	55.6	10.9	.315	1.07	4.51	5.47	17.5
32	Large	480	28.6	19.8	60.6	59.1	16.3	.145	.600	5.95	5.81	2.50
33	Large	641	30.7	21.3	68.4	61.2	21.5	.077	.366	6.72	6.01	11.7
34	Large	795	30.5	21.2	67.6	62.9	26.7	.084	.445	6.64	6.18	7.51
35	Medium	128	32.1	22.2	73.8	69.2	1.86	.592	.812	3.14	2.94	6.66
36	Medium	191	34.6	24.0	83.8	80.0	2.77	.490	.824	3.56	3.40	4.74
37	Medium	250	38.0	26.3	98.2	87.4	3.63	.375	.724	4.17	3.71	12.4
38	Medium	312	37.3	25.8	95.2	93.2	4.52	.394	.850	4.04	3.96	2.20
39	Medium	481	40.3	28.0	108.2	104.4	6.97	.304	.820	4.60	4.44	3.63
40	Small	65.3	27.2	18.9	55.6	53.3	0.53	1.44	1.04	1.33	1.27	4.37
41	Small	97.9	28.8	19.9	61.5	67.3	0.80	1.31	1.17	1.47	1.61	8.66
42	Small	130	32.6	22.6	75.8	77.8	1.05	1.08	1.11	1.81	1.86	2.53
43	Small	163	35.5	24.6	87.5	87.5	1.33	.934	1.08	2.09	2.09	1.12
44	Small	216	35.7	24.8	88.3	99.8	1.77	.921	1.23	2.11	2.38	11.5
45	Small	269	37.7	26.1	97.0	109.3	2.20	.828	1.24	2.32	2.61	11.3

Tube Type: Finned
Tube Angle: 60°

Run No.	Particle Size	G	$q/\Delta T_{av}$	h_{ff}	h_f	h_{corr}	Re	F	F/Re^a	Nu_{exp}	Nu_{corr}	% Dev.
46	Large	326	23.0	15.9	41.7	44.0	10.9	.380	1.29	4.10	4.33	5.33
47	Large	481	25.6	17.8	50.1	48.5	16.3	.259	1.07	4.92	4.76	3.35
48	Large	641	26.1	18.1	51.9	51.3	21.5	.236	1.13	5.10	5.04	1.09
49	Large	795	28.0	19.4	58.5	53.5	26.7	.165	.879	5.75	5.26	9.25
50	Medium	128	22.5	15.6	40.2	41.0	1.86	1.16	1.59	1.71	1.74	2.06
51	Medium	164	24.8	17.2	49.8	50.2	2.77	.933	1.57	2.12	2.13	0.84
52	Medium	250	26.5	18.4	53.3	56.9	3.63	.867	1.67	2.26	2.42	6.36
53	Medium	315	29.8	20.6	65.0	62.5	4.52	.687	1.48	2.76	2.65	4.03
54	Medium	481	32.3	22.4	74.7	74.0	6.97	.570	1.53	3.17	3.14	0.98
55	Small	65.2	16.0	11.1	23.0	25.1	0.53	2.79	2.02	0.55	0.60	8.47
56	Small	97.8	20.3	14.1	34.0	33.5	0.80	2.11	1.88	0.81	0.80	1.39
57	Small	129	22.5	15.6	40.3	40.2	1.05	1.85	1.90	0.96	0.96	0.19
58	Small	164	24.9	17.2	47.8	46.8	1.33	1.62	1.87	1.14	1.12	2.21
59	Small	217	26.7	18.5	54.0	55.6	1.77	1.46	1.95	1.29	1.33	2.79
60	Small	271	28.7	19.9	61.0	62.8	2.20	1.31	1.95	1.46	1.50	2.88

Tube Type: Finned
Tube Angle: 90°

Run No.	Particle Size	G	$q/\Delta T_{av}$	h_{ff}	h_f	h_{corr}	Re	F	F/Re^a	Nu_{exp}	Nu_{corr}	% Dev.
61	Large	327	22.9	15.9	41.5	46.3	10.9	.383	1.30	4.08	4.55	10.4
62	Large	480	23.1	16.0	42.2	50.6	16.3	.372	1.54	4.14	4.97	16.6
63	Large	641	24.8	17.2	47.5	53.3	21.5	.292	1.40	4.67	5.24	10.9
64	Large	795	25.3	17.5	49.2	55.4	26.7	.270	1.44	4.83	5.45	11.3
65	Medium	128	24.1	16.7	45.3	45.6	1.86	1.03	1.41	1.92	1.94	0.70
66	Medium	190	28.1	19.4	58.9	55.2	2.77	.778	1.31	2.50	2.35	6.62
67	Medium	250	30.6	21.2	68.0	62.2	3.63	.653	1.26	2.89	2.64	9.36
68	Medium	312	32.0	22.2	73.5	67.9	4.52	.556	1.27	3.12	2.88	8.29
69	Medium	481	34.4	23.8	83.0	79.5	6.97	.489	1.32	3.53	3.38	4.39
70	Medium	641	37.5	26.0	96.0	----	----	---	----	----	----	----
71	Small	65.2	18.2	12.6	27.3	29.1	0.53	2.48	1.80	0.65	0.69	6.06
72	Small	97.8	24.8	17.2	47.5	38.4	0.80	1.63	1.46	1.13	0.92	23.6
73	Small	129	29.6	20.5	64.4	45.8	1.05	1.26	1.29	1.54	1.09	40.6
74	Small	163	28.1	----	----	----	----	---	----	----	----	----
75	Small	217	31.0	21.5	69.5	62.4	1.77	1.17	1.56	1.66	1.49	11.3
76	Small	271	31.6	21.9	71.9	70.2	2.20	1.12	1.68	1.71	1.69	2.41
77	Small	409	33.5	23.2	79.0	----	----	---	----	----	----	----

Tube Type: Bare
Tube Angle: 0°

Run No.	Particle Size	G	$q/\Delta T_{av}$	h_b	h_{corr}	Re	F	F/Re^a	Nu_{exp}	Nu_{corr}	% Dev.
78	Large	326	6.79	73.8	72.0	10.9	.037	.066	7.25	7.07	2.56
79	Large	485	6.63	72.2	72.6	16.3	.049	.095	7.09	7.13	0.54
80	Large	641	6.55	71.3	72.9	21.5	.054	.114	7.00	7.16	2.19
81	Large	795	6.57	71.4	73.3	26.7	.054	.119	7.01	7.20	2.56
82	Medium	128	11.4	124	126	1.86	.228	.265	5.27	5.37	1.94
83	Medium	191	11.9	129	130	2.77	.201	.257	5.48	5.52	0.80
84	Medium	250	12.1	132	132	3.63	.186	.254	5.61	5.63	0.36
85	Medium	312	12.4	135	134	4.52	.170	.245	5.74	5.69	0.72
86	Medium	481	13.0	141	137	6.97	.143	.227	5.99	5.84	2.58
87	Medium	---	----	----	----	----	----	----	----	----	----
88	Small	65.2	11.2	122	130	0.53	.648	.556	2.91	3.12	6.53
89	Small	97.8	11.5	125	139	0.80	.623	.590	2.99	3.33	10.3
90	Small	129	12.4	135	145	1.05	.558	.565	3.44	3.47	6.94
91	Small	163	12.4	134	150	1.33	.563	.603	3.20	3.59	10.9
92	Small	217	13.0	141	156	1.77	.520	.597	3.37	3.73	9.80
93	Small	269	13.2	144	161	2.20	.501	.605	3.44	3.83	10.3
94	Small	---	----	----	----	----	----	----	----	----	----

Tube Type: Bare
Tube Angle: 30°

Run No.	Particle Size	G	$q/\Delta T_{av}$	h_b	h_{corr}	Re	F	F/Re^a	Nu_{exp}	Nu_{corr}	% Dev.
95	Large	326	7.07	76.9	70.4	10.9	.016	.029	7.55	6.92	9.26
96	Large	485	6.68	72.6	71.1	16.3	.046	.089	7.13	6.99	2.06
97	Large	641	6.44	70.0	71.5	21.5	.064	.134	6.88	7.03	2.13
98	Large	795	6.11	66.4	72.0	26.7	.093	.205	6.52	7.07	7.73
99	Medium	128	10.7	116	117	1.86	.270	.313	4.93	4.95	0.52
100	Medium	191	10.9	118	121	2.77	.256	.327	5.01	5.13	2.20
101	Medium	250	11.6	126	123	3.63	.214	.292	5.35	5.24	2.11
102	Medium	312	11.6	126	125	4.52	.211	.304	5.35	5.32	0.62
103	Medium	481	11.9	130	129	6.97	.190	.303	5.52	5.49	0.65
104	Small	65.7	11.5	125	110	0.53	.628	.539	2.99	2.64	13.1
105	Small	97.8	11.8	128	119	0.80	.604	.572	3.06	2.85	7.42
106	Small	129	12.6	137	125	1.05	.547	.553	3.27	2.98	9.69
107	Small	164	12.4	135	130	1.33	.557	.596	3.22	3.11	3.73
108	Small	217	13.1	143	136	1.77	.510	.584	3.42	3.25	5.02
109	Small	271	13.9	151	141	2.20	.465	.562	3.61	3.36	7.46

Tube Type: Bare
Tube Angle: 45°

Run No.	Particle Size	G	$q/\Delta T_{av}$	h_b	h_{corr}	Re	F	F/Re^a	Nu_{exp}	Nu_{corr}	% Dev.
110	Large	326	6.36	69.1	67.0	10.9	.072	.128	6.79	6.58	3.08
111	Large	485	5.84	63.5	68.0	16.3	.118	.231	6.24	6.68	6.67
112	Large	641	5.44	59.2	68.6	21.5	.158	.328	5.81	6.74	13.7
113	Large	790	5.08	55.2	69.1	26.7	.199	.438	5.42	6.79	20.2
114	Medium	128	9.78	106	98.4	1.86	.328	.381	4.50	4.18	7.73
115	Medium	193	8.84	96.0	103	2.77	.392	.501	4.08	4.38	6.83
116	Medium	250	9.91	108	106	3.63	.312	.424	4.59	4.51	1.70
117	Medium	312	10.1	110	108	4.52	.297	.426	4.67	4.61	1.44
118	Medium	481	10.2	110	113	6.97	.294	.468	4.67	4.81	2.78
119	Small	65.2	9.98	108	79.7	0.53	.751	.645	2.58	1.90	35.5
120	Small	97.8	10.9	119	87.4	0.80	.663	.628	2.84	2.09	36.2
121	Small	129	11.2	122	92.6	1.05	.639	.647	2.91	2.21	31.7
122	Small	164	12.0	130	97.4	1.33	.587	.628	3.11	2.33	33.4
123	Small	217	12.2	133	103	1.77	.565	.648	3.18	2.46	28.9
124	Small	271	12.2	133	107	2.20	.561	.678	3.18	2.56	23.9

Tube Type: Bare
Tube Angle: 60°

Run No.	Particle Size	G	$q/\Delta T_{av}$	h_o	h_{corr}	Re	F	F/Re^a	Nu_{exp}	Nu_{corr}	% Dev.
125	Large	326	7.28	79.1	70.4	10.9	.002	.003	7.77	6.91	12.4
126	Large	485	6.84	74.4	71.1	16.3	.033	.064	7.31	6.99	4.59
127	Large	641	6.48	70.4	71.5	21.5	.061	.128	6.91	7.03	1.57
128	Large	795	6.36	69.2	72.0	26.7	.071	.156	6.80	7.07	3.84
129	Medium	128	9.34	102	117	1.86	.354	.410	4.33	4.95	12.5
130	Medium	191	11.2	122	121	2.77	.235	.300	5.18	5.13	1.12
131	Medium	250	11.7	128	123	3.63	.205	.279	5.44	5.24	3.73
132	Medium	312	12.5	136	125	4.52	.166	.239	5.78	5.32	8.60
133	Medium	481	12.4	135	129	6.97	.168	.268	5.74	5.49	4.52
134	Small	65.2	10.2	111	111	0.53	.727	.624	2.65	2.64	0.40
135	Small	97.8	10.5	114	119	0.80	.699	.663	2.72	2.85	4.33
136	Small	129	11.4	124	125	1.05	.626	.633	2.96	2.98	0.71
137	Small	164	12.0	130	130	1.33	.587	.628	3.11	3.11	0.11
138	Small	217	12.5	136	136	1.77	.548	.628	3.25	3.25	0.12
139	Small	271	13.1	143	141	2.20	.506	.611	3.42	3.36	1.77

Tube Type: Bare
Tube Angle: 90°

Run No.	Particle Size	G	$q/\Delta T_{av}$	h_b	h_{corr}	Re	F	F/Re^a	Nu_{exp}	Nu_{corr}	% Dev.
140	Large	326	7.29	79.3	72.0	10.9	.0006	.001	7.79	7.07	10.2
141	Large	485	6.88	74.8	72.6	16.3	.030	.059	7.35	7.13	3.04
142	Large	641	6.51	70.7	72.9	21.5	.059	.123	6.94	7.16	3.01
143	Large	795	6.27	68.2	73.3	26.7	.079	.173	6.70	7.20	6.93
144	Medium	128	11.6	126	126	1.86	.218	.253	5.35	5.37	0.35
145	Medium	197	12.1	132	130	2.77	.188	.239	5.61	5.52	1.51
146	Medium	250	12.4	135	132	3.63	.173	.236	5.74	5.63	1.90
147	Medium	312	12.4	135	134	4.52	.170	.245	5.74	5.69	0.72
148	Medium	481	12.3	134	137	6.97	.172	.274	5.70	5.84	2.51
149	Small	65.2	10.2	111	131	0.53	.727	.624	2.65	3.12	15.0
150	Small	97.8	11.1	121	139	0.80	.649	.615	2.89	3.33	13.1
151	Small	129	12.5	136	145	1.05	.556	.559	3.25	3.47	6.25
152	Small	164	14.0	153	150	1.33	.463	.495	3.65	3.59	1.75
153	Small	217	14.5	157	156	1.77	.441	.505	3.75	3.73	0.43
154	Small	271	14.7	160	161	2.20	.424	.512	3.82	3.83	0.33

Tube Type: Bare
Tube Angle: 90°

Run No.	Particle Size	G	$q/\Delta T_{av}$	h_b
155	Large	326	6.82	74.1
156	Large	485	6.34	68.9
157	Large	641	5.98	65.0
158	Large	795	6.16	66.9
159	Medium	128	10.3	112
160	Medium	191	11.2	122
161	Medium	250	11.8	128
162	Medium	312	12.8	139
163	Medium	481	12.7	138
164	Small	65.2	9.10	99
165	Small	97.8	9.69	105
166	Small	129	11.6	126
167	Small	164	12.4	135
168	Small	217	13.8	150
169	Small	271	14.4	157

In Runs 155 through 169 the temperatures were averaged using the finned tube equation. The h_b's for these runs are in reasonable agreement with h_b's for Runs 140-154 (7% deviation) which were calculated using the simple equation for averaging: $T_{av} = 1/3(T_1+T_2+T_3)$.

Tube Type: Copper-clad Finned
Tube Angle: 0^{o}

Run No.	Particle Size	G	$q/\Delta T_{av}$	h_{ff}
170	Large	327	31.4	31.8
171	Large	485	33.4	33.9
172	Large	641	32.5	33.0
173	Large	795	34.8	35.3
174	Medium	128	40.0	40.6
175	Medium	191	44.5	45.2
176	Medium	250	46.7	47.4
177	Medium	315	47.8	48.5
178	Medium	481	50.0	50.8
179	Small	65.2	36.7	37.2
180	Small	97.8	38.4	39.0
181	Small	129	41.5	42.1
182	Small	164	45.7	46.3
183	Small	217	42.5	48.2
184	Small	271	49.3	50.1

MONTANA STATE UNIVERSITY LIBRARIES
3 1762 10015443 2

N378
Sch43
cop.2

Schmall, Rodney A.
The effect of orientation on heat transfer coefficients...

NAME AND ADDRESS
INTERLIBRARY LOAN
Purdue Univ
Lafayette, Ind
6-24-
INTERLIBRARY
3-31
2 WEEKS USE INTERLIBRARY
Frey 103

N378
Sch43
cop. 2